UNIVERSITY OF AMSTERDAM

**MSc physics and astronomy**

THEORETICAL PHYSICS

**Master thesis**

---

# Universality in one-dimensional models displaying self-organized criticality

---

by

**Ernst Ippel**
**10437118**

November 15, 2018
60 ECTS

Institute for theoretical physics Amsterdam

*Supervisor:*
Prof. Dr. B. NIENHUIS

*Second assessor:*
Dr. J. VAN WEZEL

## Abstract

Throughout the years, the concept of self-organized criticality has established itself as one of the most promising explanations of the occurrence of self-similar fractal structures and complexity in nature. In this thesis, we will first give a short reminder of criticality in second-order phase transitions, after which the concept of self-organized criticality is introduced and a brief overview of self-organized criticality in one dimension is given. We then proceed by analysing various one-dimensional, slowly driven sandpile models, all of which are governed by different stochastic toppling rules. Under these dynamical rules, which are defined as either being local or nonlocal, and limited or unlimited, the models quickly evolve towards a steady state which is characterized by the occurrence of avalanches of varying size. These avalanches do not necessarily have a characteristic scale, and possibly display power-law behaviour in the frequency of their occurrence. Indeed, we find that three of our models exhibit critical behaviour in the form of distributions of avalanches following a power-law, all of which are characterized by different scaling exponents. Furthermore, we find certain critical properties intrinsic to the steady state of both the local-, and nonlocal-unlimited model. Lastly, we investigate whether the critical behaviour emerging through the dynamics of our models is universal between a class of different models. This is done by introducing a flow-parameter, with which we flow from one model to the other. We find that the critical behaviour emerging in the nonlocal-limited model is indeed universal between a class of different models, where the universality class to which these models belong can be characterized by a set of four critical exponents.

# Contents

# 1 Introduction

One of the main characteristics of equilibrium systems undergoing a second-order phase transition, is the occurrence of fluctuations over all length and time scales. To describe this phenomenon, one thus requires a theory which is scale-invariant. Consequently, the research on systems undergoing such phase transitions gained a lot of interest among physicists throughout the years, which resulted in a considerable amount of insights into the associated physics, and was accompanied by the development and generalization of some theories and solving methods like mean field theory and the renormalization group. This, in turn, led to numerous breakthroughs in the area of condensed matter physics and the science of materials, and the methods developed even reached into other disciplines, like biology and economics. Studying and understanding the behaviour displayed by systems at a second-order phase transition has thus been proven to be of great value for the development of new physics and a better understanding of interactions within various materials. This behaviour is most commonly referred to as *critical* behaviour. Although in general the term *criticality* pertains to the description of these second-order phase transitions, another concept, in which critical behaviour seemed to emerge on its own without the necessity of undergoing such phase transitions, was put forward in 1987. This concept was termed as *self-organized criticality* (SOC), and in the following years, a variety of models, all characterized by some form of self-organiziation of criticality, were studied extensively in an effort to classify them according to their critical behaviour, analogous to the classification of equilibrium models displaying a second-order phase transition. This classification is carried out by grouping the models according to certain macroscopic properties that are independent of the dynamical details of these systems, and the resulting classes are called *Universality classes*. Even though this classification is reasonably well-established for models undergoing a second-order phase-transition, the classification of models displaying self-organized criticality is not established as such. In this thesis, the self-organization of criticality will be investigated in certain one-dimensional sandpile models, after which some conclusions about the existence of universality in these models will be drawn. Moreover, the question of whether the critical behaviour in these models emerges solely from the dynamics, or if there also exist some critical properties intrinsic to the steady states themselves, will be addressed.

## 1.1 Criticality and self-organized criticality

The term *critical behaviour* is thus most commonly used to refer to the behaviour displayed by thermodynamic systems that are undergoing a second order, or continuous, phase transition. However, the discovery of other phenomena displaying critical behaviour, and in particular that of self-organized criticality, has broadened its use. Although critical behaviour emerges both in models at a phase transition and models displaying self-organized criticality, there exist some fundamental differences in the way in which this behaviour manifests itself. The similarities and differences between these two manifestations of criticality will be elucidated in the following two subsections, after which an overview of the most well-known one-dimensional models displaying self-organized criticality will be given. Thereafter the concept of universality will be discussed.

### 1.1.1 Criticality in second-order phase transitions

In general, when a system ondergoes a second order phase transition, it moves from an disordered to an ordered state or vice versa. In doing so, the system either loses or gains some symmetry, where in most cases the disordered state displays a higher symmetry than the ordered state. This loss of symmetry in transitioning from the disordered to ordered state is called *spontaneous symmetry breaking*, and can often be parameterized by some order parameter, like the net magnetization in ferromagnetic systems, the difference in density for liquid-gas transitions or the electric polarization in ferroelectric materials. The order parameter is thus a measure of the degree of order, and increases continuously when transitioning from the disordered to the ordered state. In general, its value is zero in the disordered state, and non-zero in the ordered state. The point at which the system transitions from a disordered to an ordered state, is called a *critical point* or state. This critical point is reached when certain control-parameters, like temperature or pressure, are set to very precise values, i.e. their critical values. One of the main characteristics of systems approaching their critical state, is the development of long range order. In the disordered state, correlations over long distances are absent, and the correlation length is finite. As the control-parameters are adjusted to their critical value, this correlation length diverges, and correlations will form over all length scales up to the size of the system itself. In addition to the divergence of the correlation length, there often also exist other thermodynamic quantities, like the heat capacity or the magnetic susceptibility, which diverge near the critical point. These divergences can be represented as a discontinuity of the corresponding quantities at the critical point, characterizing the indistinguishability of the two phases in the critical phase. The origin of the adjective *second-order* comes from the order of the appropriate derivative of the free energy at which these kind of discontinuities occur. This can be seen through the order parameter, which, in the case of magnetism in ferromagnetic systems for example, is given by the first order derivative of the free energy with respect to the external magnetic field. First-order phase transitions are characterized by a discontinuity in the first order derivative of the free energy, whereas in second-order phase transitions, this first order derivative is continuous across the transition, but the second order derivative displays a discontinuity. The thermodynamic quantities mentioned above are thus given by the appropriate second order derivative of the free energy, and the discontinuity in these second order derivatives signals that the corresponding quantities diverge near the critical point.

We can represent the divergence of the correlation length $\xi$ and thermodynamic quantities like the magnetic susceptibility $\chi$ and heat capacity $C_v$ in terms of power-laws of the relevant control parameter. If we take the temperature $T$ as the control parameter for example, and let $T_c$ be its critical value, the divergence of these quantities can then be depicted as follows

$$\xi \propto |T - T_c|^{-\alpha}, \quad \chi \propto |T - T_c|^{-\nu}, \quad C_v \propto |T - T_c|^{-\mu}, \tag{1.1.1}$$

where $\alpha$, $\nu$ and $\mu$ are so-called *critical exponents*, which have positive value. In general, there is a small set of these, not necessarily independent, critical exponents associated with a phase transition. The concept of universality arises from the observation that phase transitions in completely different systems often occupy the same set of critical exponents.

In addition to the power-law behaviour in Eq.(1.1.1), the correlations between the microscopic variables defining the system often follow a power-law decay as function of distance at the critical point. The power-law behaviour of these quantities at a phase transition illustrates the scale-invariant behaviour of the system at the critical point. Where initially interactions only occur at microscopic scales, fluctuations of all length scales arise at a phase transition, and a scale-invariant theory is required to describe the phenomenon. Moreover, the microscopic variables become insignificant in the description of critical behaviour, which suggest that phase transitions can be classified into a few universality classes according to this macroscopic behaviour. To summarize, critical behaviour in second-order phase transitions is thus in general characterized by a diverging correlation length, power-law divergences of certain thermodynamic quantities, a power-law decay of correlations between the microscopic variables, and emerges only from the precise fine-tuning of the relevant control parameters.

### 1.1.2 Self-organized critical behaviour

Criticality in second-order phase transitions thus arises when certain control-parameters are set to very precise critical values. However, physicists noticed that a wide variety of natural phenomena display self-similar structures over a large range of different spatial and temporal scales, seemingly without the need for this precise fine-tuning of control parameters. Some of the most striking examples are earthquakes, the forming of mountains, solar flares, the spreading of forest-fires and coastlines. Although these phenomena thus exhibit certain critical properties, no required fine-tuning is needed in order to obtain these self-similar, or scale-invariant structures. It thus seems that, in nature, criticality, under widely different circumstances, can organize on its own. In an effort to model these observations, Per Bak et al. published a paper in 1987 [1], in which they coined the term *self-organized criticality*. They introduced the Abelian sandpile model, which is a two-dimensional model in which critical behaviour emerges on its own i.e. displays self-organized criticality. This was an enormous break-through, as they possibly discovered a mechanism by which the occurrence of complexity and self-similar fractal structures in nature could be explained. The concept of self-organized criticality was introduced as a feature of dynamical non-equilibrium models which, for a wide range of initial states, organize themselves into a minimally stable state lying at a critical point. The critical point is thus an attractor of the dynamics. Still, the systems somehow have to reach this state through these dynamics, and SOC is therefore typically seen in systems which are slowly driven and have some dissipative mechanism. In general, this slow driving force pushes the system from a random initial state, in which the correlations in time and space are local, to a state displaying spatial and/or temporal scale-invariance. However, as mentioned above, contrary to real phase transitions, these "transitions" in models displaying SOC do not require a precise fine-tuning of control parameters, like temperature or pressure. The point(s) in phase space, which represent the, possibly critical, steady state, thus fulfill the role of an attractor, towards which an SOC displaying system naturally evolves. In real phase transitions, criticality is only reached when the external parameters are fixed in such a way that the state of the system lies in the vicinity of the critical fixed point(s), and a very precise fine-tuning is thus required. If the values of these parameters initially lie far from their critical value, no critical behaviour will be observed, even if the system is perturbed or other parameters are adjusted. As in systems at a second-order

phase transition, there exist certain quantities in models displaying SOC that exhibit power-law behaviour. In second-order phase transitions, the critical properties, like the diverging correlation length or the power-law decay of the correlations, can be seen as some property intrinsic to the critical steady state. Even though this diverging correlation length and power-law decay of correlations could also be found in the steady state of the original Abelian sandpile model, this isn't necessarily the case in all models displaying self-organized criticality. On the other hand, systems displaying SOC often seem to give rise to certain critical behaviour which emerges through the dynamics rather than being some intrinsic property of the steady state. This behaviour result from the nature of the slow driving force, which often acts as a small, local perturbation of the steady state. This small perturbation can either have no effect, or can affect the steady state on arbitrary large scales. It is often observed that the effect caused by this perturbation doesn't have a characteristic scale, and that if we quantify these effects they follow a power-law distribution. Whether some critical properties are thus to be found in some sort of intrinsically critical steady state, or if the critical behaviour emerges through the dynamics of the system, is in general not known a priori for SOC-models. Furthermore, whether the critical behaviour emerging through the dynamics requires some sort of scale invariant behaviour intrinsic to the steady state, or can emerge solely from these dynamics, does not seem to be investigated anywhere in the literature. In this thesis, we will therefore investigate both the possible existence of critical properties intrinsic to the steady state, and the possible criticality in the behaviour emerging from the dynamics. Thereafter, we will also try to answer if the critical behaviour emerging through the dynamics can exist without some form of scale-invariance in the steady states.

## 1.2 Overview of one-dimensional models displaying self-organized criticality

The concept of self organized criticality was thus first introduced by Per Bak, Chao Tang and Kurt Wiesenfeld (BTW) in their paper published in 1987 [1]. In this paper it is shown that certain systems with spatial degrees of freedom, in which the local dynamics are governed by a small set of simple rules, naturally evolve towards a critical steady state, in which the correlation length diverges and the correlations decay as a power-law. This model is thus known as the *Abelian sandpile*, or *Bak-Tang-Wiesenfeld* model. In this model, a two-dimensional square lattice is considered, in which a nonnegative, finite value $z(x, y) \in \mathbb{Z}$ is assigned to every lattice point $(x, y)$. Any site $(x, y)$ for which $z(x, y) \geq 4$ is unstable, and topples according to the following toppling rules

$$z(x, y) \to z(x, y) - 4, \tag{1.2.1}$$

$$z(x \pm 1, y) \to z(x \pm 1, y) + 1, \tag{1.2.2}$$

$$z(x, y \pm 1) \to z(x, y \pm 1) + 1, \tag{1.2.3}$$

The model can be seen as representing a sandpile, in which in general a highly unstable inital state is chosen, lying far from the attractor of the dynamics. This could for example be a state in which $z(x, y)$ is too large on all sites, exceeding some critical slope-value $z_c$. Thereafter, the dynamic rules ascertain that this state collapses until a minimally stable critical state is reached, in which the slope doesn't exceed $z_c$ anywhere. If then a single grain of sand is added to the system at a random site $(x, y)$, such that $z(x, y) \to z(x, y) + 1$, avalanches of all length scales,

and thus of all time scales, can occur. A key observation here, is the addition of a grain of sand to the system. This adding of grains of sand plays the role of a slow driving force, which pushes the system towards its steady state, and simultaneously acts as a small local perturbation. Such slow-driving forces, be it bulk or boundary driven, are a requirement for these kind of systems to show any scale-invariant, or critical behaviour. On top of the emergence of scale-invariance in the steady state, the probability distributions $P(s)$ and $P(t)$, of the occurrences of avalanches with avalanche-size $s$ and avalanche-time $t$, exhibit power-law behaviour as

$$P(s) \sim s^{-\tau}, \tag{1.2.4}$$

$$P(t) \sim t^{-\gamma}, \tag{1.2.5}$$

where $\tau$ and $\gamma$ again are critical exponents, which characterize the self-organized critical behaviour. The size $s$ and time $t$ of avalanches can be defined in multiple ways, and are often related to each other by another scaling exponent. Another popular choice for the initial state, is to start with an empty grid, i.e. a state in which no site is occupied by any grains, or $z(x, y) = 0$ $\forall\, x, y$. A potential drawback of this approach, is that the steady state first has to be reached by adding a certain amount of grains. This could perturb the data of the probability distributions of avalanches in some cases. In practise however, the time needed to reach such a steady state doesn't seem to make a significant difference on the outcoming distributions, at least in the case of one-dimensional finite systems which are not too large. Although the majority of the self-organized critical models introduced throughout the years are defined in two dimensions or higher, some models displaying self-organized criticality in one dimension were also discovered. Most of these are a variation of a select few models, of which a short overview is given below.

### 1.2.1 The BTW model

In the one-dimensional BTW sandpile model, an initially empty lattice of length $L$ is considered, to which grains of sand, or height-units $h_i \in \mathbb{Z}$ are added at random. The lattice is bounded on the left and is open on the right, so grains can only leave the system on the right. The integer heights $h_i$ thus represent the number of grains stacked on top of each other at each lattice point $i$. From these heights, a local slope between two next nearest neighbours can be defined as

$$z_i = h_i - h_{i+1}. \tag{1.2.6}$$

Dropping a grain of sand at site $i$ results in a change in the slopes as

$$z_i \to z_i + 1 \tag{1.2.7}$$

$$z_{i-1} \to z_{i-1} - 1. \tag{1.2.8}$$

This dropping of grains is continued until at some site $i$, some predefined critical slope $z_c$ is exceeded, after which the site topples a grain to its next nearest neighbour on the right, initiating an avalanche of at least size $s = 1$. Note that in this sense, the one-dimensional BTW model is a directed model, as the grains are only allowed to move towards the open boundary. Also note that, although various definitions of avalanche-size could give rise to critical behaviour, in [1] the size $s$ of an avalanche is defined as the total number of topplings that occur in between two depositions of new grains. Such a toppling at some site $i$ of one particle to its right-neighbour

can be represented by the following changes in the slopes

$$z_i \to z_i - 2 \tag{1.2.9}$$

$$z_{i-1} \to z_{i-1} + 1 \tag{1.2.10}$$

$$z_{i+1} \to z_{i+1} + 1, \tag{1.2.11}$$

and this process will continue until none of the remaining slopes exceed $z_c$. Thereafter, a new grain will be added at a random site, and the process repeats itself. An important feature of the BTW model, and of models based on these unstable grain-dynamics in general, is that this addition of new grains only takes place after all possible topplings have occurred. This is implemented as to resemble the short relaxation time of the system in comparison to the frequency of the driving force, which thus drives the system slowly from its initial state to its steady state. When this steady state hasn't been reached yet, the occurring avalanches will most likely be local and will only affect a small number of sites. After a sufficient amount of added grains, the steady state will be reached, which in general is a state in which avalanches of all sizes can occur. However, in the one-dimensional BTW model, this steady state consists of only a single stable state, in which $z_i = z_c \ \forall \ i$, meaning all $h_i$ differ by $z_c$ in descending order from closed to open boundary. When a grain is added to the system in this steady state, it will just topple until it is lost at the open boundary. Dropping a grain at a random site $i$ will then result in an avalanche of size $s = L - i + 1$, which indeed does not have any characteristic length, or time scale. However, the probability of observing an avalanche of size $s$, is $p(s) = 1/L$ for any given size $s$. The distributions of avalanche size, and time, are therefore uniform, and no power-law distributions are observed, which, since the steady state is definitely non-critical in this case, is required if one wishes to speak about SOC. Although the dynamics thus give rise to trivial avalanche-distributions in the one-dimensional case of the original BTW sandpile model, and the steady state consists of only a single non-critical state, there were a few variations on the BTW model, displaying SOC in $d = 1$ dimension, introduced in the following years.

### 1.2.2 The Kadanoff model

One of the first to introduce one-dimensional sandpile models displaying self-organized criticality was Kadanoff et al.[2]. In many aspects, these models are similar to the one-dimensional BTW model. Again a height $h_i$ is associated to every site $i$, and a slope, $z_i = h_i - h_{i+1}$, is defined. If a slope $z_i$ then exceeds the critical slope $z_c$, the site topples according to certain toppling rules. The difference between the one-dimenional BTW model, and the models introduced by Kadanoff, lies in these rules governing the dynamics of the system. Kadanoff introduces four differing models, all of which have the following toppling rule in common when the slope $z_i$ at site $i$ exceeds $z_c$

$$h_i \to h_i - n_i, \tag{1.2.12}$$

where $n_i$ is the number of grains moving to the right-neighbour(s) of site $i$. However, this number of grains $n_i$ differs per model, and depends on whether the model in consideration is limited or non-limited. Furthermore, the grains that drop can fall according to local, or nonlocal toppling rules. Limited models are defined as models in which $n_i$ is limited to take on a constant value

$$n_i = N, \tag{1.2.13}$$

whereas in non-limited models, $n_i$ grows in proportion to the slope $z_i$

$$n_i = z_i - N. \tag{1.2.14}$$

Moreover, he defines models to be local when grains only topple to their next nearest neighbour

$$h_{i+1} \to h_{i+1} + n_i, \tag{1.2.15}$$

whereas in nonlocal models, one grain is added to the $n_i$ right-neighbours of site $i$ after a toppling

$$h_{i+j} \to h_{i+j} + 1 \quad \text{for} \quad j = 1, ..., n_i. \tag{1.2.16}$$

Although each of these models displays different behaviour, they all give rise to critical behaviour of avalanche-distributions. A thing to note, is that Kadanoff makes use of multifractal scaling analysis in order to extract critical exponents from the obtained avalanche-data, as opposed to the finite-size scaling ansatz, which is more commonly used and will also be used in this thesis. The main reason for this, is that the resulting distributions could not be well-described by the finite-size scaling ansatz. Kadanoff also mentions, that all four categories of models belong to different universality classes, but is seems that this statement is only based on the observed differences in critical behaviour, and not on some investigation regarding the possible universal nature of this behaviour. He does, however, considers two models within the same category, but with adjusted parameter values, and concludes that the critical behaviour remains unchanged. Whether these models can be regarded as non-trivially different, and therewith provide convincing enough evidence to speak about universality between two different models, is up for debate.

A very similar model to the local-unlimited Kadanoff model, also displaying interesting critical behaviour in one dimension, is presented in [7]. This model is stochastically driven at a finite rate, as opposed to the BTW and Kadanoff models, which are stochastically driven at a vanishing rate, meaning no new grains are added to the system before all possible topplings have occurred. The main difference between the local-unlimited Kadanoff model and the model presented in [7], is that the heights $h_i$ are now allowed to take on real values $h_i \in \mathbb{R}$, whereas earlier only integer values were allowed. One might wonder whether this seemingly small adjustment leads to fundamentally different critical behaviour, and it turns out that indeed this is the case, as different scaling laws, power-law spectra and thus critical exponents were observed.

### 1.2.3 The Manna model

In 1991, the so-called Manna sandpile model was introduced by Manna [3]. This model is a two-state version of the BTW model, in which initially every site is either empty or occupied by a single particle. A particle is then added at a randomly chosen site, and if this site is empty, it will remain there and nothing happens. If, however, the site is occupied, the two particles will be redistributed randomly and independently among their nearest neighbours. If any of the neighbouring sites are also occupied, these sites will also redistribute their content among their neighbours until no sites are occupied by more than one particle. Although the Manna model initially was introduced in $d = 2$ dimensions only, a number of one-dimensional variations on the model were introduced [4],[5],[6],[14],[15], all displaying non-trivial critical behaviour. Note that some of these variations have two open boundaries and the particles are allowed to move in

both directions, and in this sense are thus undirected, contrary to both the BTW and Kadanoff models. In [4], an Abelian Manna model is considered, defined on several one-dimensional lattices, and power-law distributions of avalanches were observed. The model is abelian in the sense that the statistics of the occurring avalanches does not depend on the order in which unstable sites redistribute their content. Although the original Manna model is non-abelian, it is shown in [16] that the critical behaviour observed in the abelian and non-abelian version is not fundamentally different, and that in two dimensions the critical exponents coincide. In [5],[6] and [14],[15], so-called fixed-energy Manna models are studied, in which no particle creation or annihilation occurs. The number of particles, and thus the energy, or total particle density $\rho$, is conserved. In the initial state, every site $i$ is either empty or can be occupied by $n_i$ particles, i.e. $h_i \in \{0, 1, 2, ..., n_i\}\ \forall\ i$. It must be noted that in height-restricted models [15], the height $h_i$ is restricted to a certain maximum. When a site is occupied by two or more particles, it becomes an active site, otherwise it is inactive. Given some initial state with particle density $\rho$, an active site is chosen at random, and two particles at that site will independently topple randomly to one of its neighbouring sites. This can be depicted as follows

$$h_i \to h_i - 2 \tag{1.2.17}$$

$$h_{i+1} \to h_{i+1} + c_a \tag{1.2.18}$$

$$h_{i-1} \to h_{i-1} + c_b, \tag{1.2.19}$$

where $c_{a,b}$ can take on the values $c_{a,b} = 0, 1, 2$, depending on how often an adjacent site is chosen as dropping-target, and is constrained to $c_a + c_b = 2$. The transitions that may occur in these fixed-energy systems, are so-called absorbing-state phase transitions, which are characterized by a transition from a state with a random number of active sites to a state with no active sites, i.e. an absorbing state. The key lies in finding the critical particle density $\rho_c$ for which critical behaviour emerges while transitioning from the active to the absorbing state. If $\rho > \rho_c$, the so-called active-site density $\rho_a(t)$ remains relatively constant in time, and the probability of transitioning from an active to an absorbing state is so small that the system might remain in an active regime forever. If $\rho < \rho_c$, the active-site density $\rho_a(t)$ decays exponentially in time, and any given initial active state will transition to an absorbing state without displaying criticality. If $\rho = \rho_c$, the active-site density decays as $\rho_a(t) \sim t^{-\beta}$, thus following a power-law with respect to time $t$. The active site density $\rho_a(t)$ can thus be seen as a nonconserved order parameter, and the particle density $\rho$ as a control parameter; critical behaviour will only be observed when $\rho = \rho_c$. It must be noted that, in this sense, these fixed-energy Manna models thus seem to exhibit a transition which can be considered a true phase transition, contrary to the non-fixed sandpile models. Whether these fixed-energy sandpile models can be considered as displaying SOC is thus up for debate.

### 1.2.4 The Oslo ricepile model

A third model displaying SOC in $d = 1$ dimension, is the Oslo rice-pile model [8], named after the experiments done with rice grains in Oslo in 1996 [9]. These experiment were the first that were able to successfully demonstrate the existence of self-organized criticality in a controlled and replicable manner. The Oslo model is again very similar to the BTW sandpile model, except now, instead of the addition of grains at randomly chosen sites, grains are only added at site

$i = 1$. This restriction was introduced in order to mimic the experiments described in [9], in which rice grains were only added close to the vertical wall. This vertical wall is represented by the closed boundary in the model. Moreover, the value of the critical slope, $z_c^i$ , is now chosen randomly every time a site $i$ topples, and is thus not constant in time and space. In the experiments, it was observed that the slope varied along the pile, and changed in time at any given point in space along the pile. This behaviour is mimicked by introducing the non-constant slope $z_c^i$, which indeed leads to SOC, and partially manages to replicate the behaviour observed in the experiments. In both the rice-pile, and the BTW model, there is thus an occurrence of some kind of randomness. In the ricepile model, however, this randomness is implemented in the rules governing the dynamics of the system, whereas in the BTW model, it arises in the dropping of grains at random sites. The difference between this internal and external randomness respectively, leads to fundamentally different behaviour between the two models, and also differentiates the rice pile model from the Manna, and Kadanoff models.
Many variations on the rice-pile model were introduced in the past two decades [10],[11],[12],[13], all displaying SOC and avalanche distributions following power-laws with differing critical exponents. In [10],[11], certain rules are imposed to determine whether a site is regarded as active or not. Thereafter, two different threshold values $S_1, S_2$ for the slope, $z_i = h_i - h_{i+1}$, between nearest neighbours are defined. If a site $i$ is found to be active, it moves a grain to site $i + 1$ with probability $p$ if $z_i > S_1$, and with unity if $z_i > S_2$. The avalanches end when no active sites remain on the lattice, after which a new grain is added at site $i = 1$. When $p$ is taken to be either 0 or 1, the trivial BTW model is recovered. In [12], a stochastic local limited version of the rice-pile model is introduced, and in [13] a conserved, or fixed-energy version is defined to study the critical behaviour of an absorbing-state phase transition.

### 1.2.5 The forest-fire model

The fourth and last main model displaying SOC in one dimension that will be discussed here is the forest-fire model [17]. The model was initially defined on a lattice in any dimension, but it isn't clear whether this particular model also displays SOC in one dimension, as the authors do no treat the one-dimensional case. In the following years however, a few variations that were shown to display SOC in one dimension were introduced [18],[19],[20]. In [17], the spatial distribution of dissipation of fire is studied by looking at the spreading of a fire among occupied sites, mimicking the spreading of a forest-fire. This is done by starting in a state in which a site is either empty, occupied by a tree, or occupied by a burning three. Thereafter this state is updated simultaneously by the following rules: (i) Empty sites get occupied by a tree with a probability $p$. (ii) A tree ignites into a burning tree if at least one of its $2d$ nearest neighbours is occupied by a burning tree. (iii) A site occupied by a burning tree becomes an empty site. There is thus only one parameter in this model, namely the growth rate $p$ with which trees grow, and this parameter acts as the driving force of the system. The authors find a fire-fire correlation function that decays as a power-law of distance between forest-fires, accompanied by a correlation length of the form $\xi(p) \propto p^{-\nu}$. This implies that a critical steady state is thus obtained in the limit $p \to 0$, meaning that the growth rate of trees, or driving force of the system, must be sufficiently low. They also find that the spatial distribution of forest-fires follows a fractal pattern on scales smaller than the correlation length, which thus manifests itself as criticality in the limit $p \to 0$.

The one-dimensional forest-fire models described in [18],[19],[20] are very similar to this model. The main differences lie in the way in which criticality manifests itself, and in one dimension there seems to be a need for a new stochastic parameter $f$, with which not-burning trees ignite into burning trees. In all three papers, a lattice of length $L$ is considered, and criticality is obtained in the limit $f/p \to 0$. In [18], power-law behaviour was found in the distribution of sizes of holes, or clusters of empty sites, between forests, and in the distribution of sizes of clusters of burning trees. In [19], in addition to these distributions, a power-law is found in the size distribution of forests, not necessarily burning, and in [20] a power-law is found in the density of empty sites as a function of $1/f$. An interesting aspect of all forest-fire models discussed here, is that they all display critical properties intrinsic to the steady state. As mentioned above, this doesn't always seem to be the case in one-dimensional systems displaying SOC, as criticallity is often only found in the form of power-law distributions emerging through the dynamics [2],[7],[8],[10, 11, 12, 13], and is not found as some property of the steady state itself. This of course doesn't necessarily imply that the steady state is non-critical, but rather that no critical quantities belonging to the steady state have been investigated.

### 1.3 Various definitions of an avalanche

The way in which criticality arises is thus not necessarily similar in models displaying SOC. It seems that in one dimension, at least in slowly driven sandpile or ricepile models, criticality is more often found as arising from the dynamics rather than from some properties intrinsic the steady state. In dimension $d \geq 2$, the steady state often seems to exhibit certain critical properties, like the diverging correlation length and a power-law decay of correlations between the relevant variables, analogous to for example the spin-spin correlation in ferromagnetic systems at a second-order phase transition. On top of that, there may be quantities found as emerging from the dynamics that display criticality as well. This is also the case in the original two-dimensional BTW model, in which, in addition to a critical steady state, distributions of avalanches are found which display power-law behaviour as function of avalanche-size. There are, however, several ways in which this avalanche-size can be defined, and these various definitions can often by related to each other in terms of scaling laws. Commonly used definitions of avalanche-size $s$ in two dimensions are for instance: (i) Size $\mathrm{s_{top}}$, the total number of topplings that occurred during relaxation. (ii) Radius $r$, the distance between the furthest affected site and the site of origin of an avalanche. (iii) Area $a$, the number of sites affected by an avalanche. (iiii) Liftetime $T$, how long it takes for an avalanche to diminish, where every toppling, or simultaneous multitude thereof, counts as one time step. If we let $x, y \in \{\mathrm{s_{top}}, r, a, T\}$, these various definitions of avalanche-size can be related to each other as

$$\langle x \rangle \propto y^{\beta_{xy}}, \tag{1.3.1}$$

where $\beta_{xy}$ is a critical exponent that depends on the chosen definitions of $x$ and $y$. These exponents can be used in the characterization of critical behaviour, and if $\beta_{xy}$ is known for given $x$ and $y$, one can estimate the power-law behaviour of $x$ given $y$ or vice versa. For example, in the $2d$ BTW model, it is proven that $\langle \mathrm{s_{top}} \rangle \propto r^2$ and $\langle T \rangle \propto r^{5/4}$ [21]. In the analysis of the one-dimensional models presented in section (2), also various definitions of avalanche-size can be used. The total number of topplings $\mathrm{s_{top}}$, total number of particles that fall in these

topplings $s_{drop}$, timelife $T$ of an avalanche, or total number of particles that leave the system during relaxation are a few examples. In this thesis, the distributions of avalanches will be mainly analysed by using the definitions of $s_{top}$ and $T$ as avalanche-size. The total number of particles that fall, which isn't necessarily directly proportional to the total number of topplings in some of our models, will also be looked upon shortly, as there arose some seemingly contradicting features when looking at the critical behaviour arising from the distributions of $s_{top}$ versus $s_{drop}$.

## 1.4 Universality

Physicists studying widely different systems at a second-order phase transition, noticed that these systems often would display similar behaviour at their respective critical points, and that this behaviour thus seems independent of the details of the microscopic variables. The notion of *universality* arose, which states a large number of different systems, all exhibiting certain scale-invariant behaviour independent of the dynamical details, can be classified into a few classes according to this critical behaviour. As mentioned above, these classes are so-called *universality classes*, and the emerging power-law behaviour found in certain quantities of systems lying in the same universality class show equivalence in their scaling, or *critical exponents*. Systems sharing exactly the same set of critical exponents belong to the same universality class. In lower-dimensional systems, the critical exponents arising during a phase-transition can be determined with the use of the renormalization group. Systems with identical critical exponents thus exhibit similar scaling behaviour in their scale-invariant limit in the renormalization group sense. In higher-dimensional systems ($d \geq 4$), the use of mean-field theory is often sufficient in order to achieve analytical results. The observation that a variety of completely different systems can share the same set of critical exponents, and thus show similar scaling behaviour, has also been made in models displaying self-organized criticality. Although certain universality classes do exist for models displaying SOC, the classification is not as well-established as in systems undergoing a continuous phase-transition.

### 1.4.1 Universality classes

A universality class is thus a set of models which exhibit similar scaling behaviour and scaling exponents at their respective critical points. In general, universality classes are dimension-dependent, meaning that the same model expressed in different dimensions will not lie in the same universality class. Models which exhibit second-order phase transitions in multiple dimensions often form a family of universality classes, one for each dimension. In addition to the dimension of the models, it is also believed that the universality class is determined by the microscopic symmetries of the systems. Some of the most well-known universality classes for systems diplaying second-order phase transition are the classes containing the: Ising model, the Ashkin-Teller model (two coupled Ising models), percolation models and the q-state Potts model.

### 1.4.2 Universality in self-organized critical models

The concept of universality in the context of self-organized criticality is thus less well-established. To date, there only seem to be a few universality classes of models displaying SOC identified.

It must also be noted that, in systems exhibiting second-order phase transitions, there exists a somewhat standard set of critical exponents based on which universality is defined. This set of critical exponents doesn't seem to be as well-defined in SOC-models, and it is therefore of importance to explicitly state with which set of critical exponents the universality class is characterized for every individual case. There are, however, certain properties of systems which can be used to define two models as different when one wishes to make statements about universal behaviour between different models. These properties are: (i) Abelian vs. non-abelian. (ii) Directed vs. undirected. (iii) Deterministic vs. stochastic. (iiii) Conservative vs. non-conservative. If the critical behaviour emerging in two models, that differ in at least one of these properties, is described by the same set of critical exponents, one can assign them to the same universality class without having to argue about whether the models are fundamentally different or not. If this is not the case, one can still assign two differing models displaying similar behaviour to the same universality class, but the question of whether these models are really different is harder to answer. Some broadly accepted universality classes of SOC-models are the classes of the stochastic, and deterministic, directed sandpile models, the Manna universality class, the BTW class in $d = 2, 3, 4$ dimensions and the conservative OFC-model of earthquakes. In one dimension however, the number of reasonably well-established universality classes is limited to one, namely, the local linear interface universality class, which is a class of directed stochastic sandpile models to which a few completely different models also seem to belong. This local linear interface class is characterized by a set of critical exponents that describe the behaviour arising through the dynamics rather than describing some properties intrinsic to the steady state. There are also two other classes conjectured [22], but these conjectures only seem to be based on the discovery of two models with new critical exponents, and no further investigations are done. In this thesis, the critical behaviour of the investigated models is also mainly found as emerging through the dynamics; in the form of avalanche-distributions following power-laws with avalanche-size. We show the existence of a new universality class of one-dimensional sandpile models based on this behaviour, which is characterized by a set of four avalanche-exponents.

# 2 The models

The models that will be investigated in this paper are based on those introduced by Amaral & Lauritsen [22]. Initially, an attempt was made to replicate these models. This, however, turned out to be quite difficult, as the information provided by Amaral et al. regarding the implementations of their models is limited to such an extent that this replication became seemingly impossible. Inevitably, some differences arose in some of the models discussed, of which the causes cannot be explained due to this shortage of information. These differences also led to different critical behaviour in some models, which expressed itself in terms of differing values in the corresponding critical exponents. Although our models are thus based on those presented in [22], they are not necessarily equal in every aspect, and a new analysis of all models was thus required. In the following subsections, we will describe our models, and implementations thereof, as precise as possible in order to avoid possible confusion in future works.

## 2.1 Amaral rice-pile models

The models that will be analysed in this thesis are one-dimensional directed sandpile models with stochastic toppling rules, all of which are a variation of the so-called "Oslo ricepile model" presented in [8] and described in section (1.2). Four variations of this model will be investigated, which are differentiated based on their dynamical rules being local versus nonlocal, and limited versus unlimited. All models are defined on a lattice of length $L$, with a closed boundary, or wall, at site $i = 0$, and an open boundary at site $i = L + 1$. Particles always move from closed to open boundary, and leave the system at site $i = L + 1$. The addition of new particles to the system is always done, one at a time, at site $i = 1$, and this addition acts as the external driving force. After a particle-deposition, relaxation of the state occurs, which thus always takes place in between the addition of two new particles. During relaxation, all *active* sites on the lattice are considered. A site $i$ is regarded active if, during the previous timestep, one of the following situations occurred: (i) Site $i$ received a particle from its left-neighbouring site $i-1$ for the local models, or sites $i-j$, $j = 1, 2, ...N$ for the nonlocal models, where $N$ is defined in Eq.(2.1.2). (ii) Site $i$ toppled one or more particles to site $i + 1$. (iii) Site $i + 1$ toppled one or more particles to site $i + 2$. Note that a single updating of active sites is defined as one timestep. When a site $i$ is active, and the local slope $z_i = h_i - h_{i+1}$ exceeds some critical slope $z_c$, the site $i$ topples one or several particles to its right-neighbour(s) with a probability $p(z_i)$. This probability is defined as folllows

$$p(z_i) = min\{1, g \cdot (z_i - z_c)\}, \tag{2.1.1}$$

where $min\{\}$ is the minimum function, and $g \leq 1$ is a parameter. This probability models the friction between particles, as a large variation in slopes in the stable configurations was observed in the experiments done on ricepiles [9], and the parameter $g$ is used to represent the strength with which gravity acts on the packing configurations.

The number of particles $N$ that fall in a single toppling event depends on the model at hand, and differs when considering the *limited* versus the *unlimited* model. The following toppling rules are defined for these cases

$$N = \begin{cases} N_0, & (l) \\ z_i - z_c, & (u) \end{cases} \tag{2.1.2}$$

where $(l)$ stands for limited and $(u)$ for unlimited. If then an active site topples, these $N$ particles are redistributed according to either the *local* or *nonlocal* rules:

$$\begin{aligned} h_{i+1} &\to h_{i+1} + N, \quad (L) \\ h_{i+j} &\to h_{i+j} + 1, \quad j = 1, 2, ...., N \quad (N) \end{aligned} \tag{2.1.3}$$

where $(L)$ stand for local, and $(N)$ for nonlocal. Naturally, the models being investigated are thus the local-limited model $(Ll)$, the local-unlimited model $(Lu)$, the nonlocal-limited model $(Nl)$ and the nonlocal-unlimited model $(Nu)$. Notice that the rules in Eq.(2.1.2) and Eq.(2.1.3) are similar to those defined in Kadanoff et al. [2], except now the randomness is implemented in the stochastic critical slope as opposed to the randomly chosen site where the particle-deposition takes place. Also note that $z_L = h_L$, and particles that topple from site $i = L$ are lost at the open boundary.

## 2.2 Implementations

The simulations of the models always take place in the slowly driven limit, meaning the frequency of the external driving force is low compared to the relaxation time of the steady state. As mentioned above, this is implemented by only adding new particles to the system when all possible topplings have occurred and no active sites remain, making sure the time in between deposition of two particles is thus long compared to the relaxation time. When doing the simulations, we always start with an empty state, do one run of the simulation and observe the minimally stable final state which resulted from the dynamics. From then on, this ending-state, or a state very similar to this one, will be used as the starting point of following simulations. We do this to make sure we either start in, or very near, the attractor of the dynamics, in order to minimize the disturbance of the data due to the unknown number of time steps it might take to reach this attactor when starting from the empty state. During every simulation, we drop at least $10^7$ particles at site $i = 1$ in between relaxations, where every deposition can lead to an avalanche of arbitrary finite size up to some power $\sim L^\nu$ of the systemsize $L$. Note that, because of the probability in Eq.(2.1.1), not necessarily every deposition of a particle will result in an avalanche. However, $10^7$ depositions of particles turned out to be more than enough in order to sufficiently analyse the data emerging from the dynamics. In this analysis, we will be looking at the distributions of the frequency of occurrences of avalanches with some predefined avalanche-size $s$. These distributions turn out to be well described by the following power-law form

$$P(s, L) = s^{-\tau} f(s/L^\nu), \tag{2.2.1}$$

where $\tau$ and $\nu$ are critical exponents, and $f(s/L^\nu)$ is some unknown scaling function. However, because of noise, running-time, and bias in the representation of binned data, we choose to analyse our data with the use of the integrated, or cumulative, distribution of Eq.(2.2.1),

which results in a change in the exponent of $s$, as $s^{-\tau+1}$. The form of Eq.(2.2.1) is known as a finite-size scaling ansatz, which will be elucidated further in section (4.1). The definition of avalanche-size $s$ will be taken as the total number of topplings $\mathrm{s_{top}}$ that occur in between two particle-depositions. Furthermore, we will also use the lifetime $T$ of an avalanche, which is defined as the total number of declarations of new active sites during relaxation. Lastly, we will shortly consider the total number of particles $\mathrm{s_{drop}}$ that fall in all toppling events during relaxation. Amaral initially uses the total potential energy dissipated in between two depositions as the definition of avalanche-size, which is defined in [9]. Thereafter, it is stated that no differences in critical exponents arise when defining an avalanche according to the total number of topplings versus the dissipated potential energy, as, on average, a toppling event dissipates a constant amount of potential energy. This, however, doesn't seem to be the case in the unlimited models analysed in this thesis, and some questions about consistency arose from an attempt to find the reason for this difference between our models and those introduced by Amaral et al. These seemingly inconsistent features will be discussed in section (6.1).

The system-sizes $L$ that will be used, depend on the properties that are investigated, but system-sizes up to $L = 3200$ will be used to extract accurate estimates of the critical exponents from the data. With an eye to the investigation of universality in our models discussed in section (5), we are also interested in the ranges of the values of the parameters $g$, $N_0$ and $z_c$ under which the critical behaviour of the systems remains unchanged. Investigations show, that the critical avalanche-exponents, and therewith the critical behaviour emerging from the dynamics, do not change significantly under the following ranges of the parameter-values: $g = 1/6, ..., 1/12$ ($g = 1/4, ..., 1/12$ for the local-limited case), $N_0 = 1, ..., 4$ ($N_0 = 2, .., 4$ for the nonlocal case), and $z_c = 1, ..., 6$. We will explicitely state which values are used in every single analysis. Also note that, in all models, with the exception of the local-unlimited model, well-behaved power-law distributions as function of avalanche-size $s$ are observed, where $s$ is thus taken as $\mathrm{s_{top}}$, $\mathrm{s_{drop}}$ and $T$. The distribution of the local-unlimited model is not convincing enough, at least when the avalanche-size is defined as the total number of topplings during relaxation, or timelife of an avalanche. When taking the total number of particles that fall during relaxation, the distribution is more convincing, as a straight line is observed in the log-log plot. However, this distribution doesn't exhibit scaling after a certain system size, which implies that we cannot consider it as a real power-law and the behaviour doesn't hold in the thermodynamic limit. Although we thus didn't find convincing critical behaviour in terms of avalanche-distributions following a power-law in the local-unlimited model, this doesn't necessarily imply no proper power-law behaviour can be found with other definitions of avalanche-size.

### 2.2.1 Parallel versus sequential updating

The method with which the active sites are updated, and therewith the order in which sites topple, turned out the be one of the main obstacles in replicating Amaral's models. Whether one uses sequential, or parallel updating, leads to significant differences in the emerging critical behaviour, and in some cases can even lead to the absence thereof. The reason for this, is that when sequential updating of active sites is used, active sites that are updated first can affect active sites that still need to be updated.

When parallel updating is used, the set of active sites $Y$ is checked in parallel, or simultaneously, and every site $i \in Y$ topples with a probability $p(z_i)$ as defined in equation (2.1.1). Now let $X \subseteq Y$ be the subset of active sites that are determined to topple. When this set $X$ is determined, $Y$ will become the empty set, and a set of new active sites $Y'$, based on $X$, is formed according to the rules defined in subsection (2.1). However, when parallel updating is used, no site $i \in X$ will topple until *after* the whole set $X$ is formed. This is what is meant with simultaneously checking all active sites, as now no active site can affect the future of other active sites during a single timestep. If $X$ is then formed, all sites $i \in X$ topple simultaneously, after which $X$ will become the empty set. Thereafter, the empty set $Y$ becomes equal to the new set $Y = Y'$ of active sites, the new set $Y'$ becomes the empty set, and the process repeats itself until *no active sites* remain. All three sets will thus be empty at the end of an avalanche, and the size of the avalanche is determined by either the total number of sites $\mathrm{s}_{\mathrm{top}}$ that were added to the set $X$ during this time, or the total number $T$ of occurrences of the set $Y'$ of new active sites. When the size of an avalanche is registered, a new particle will be dropped at site $i = 1$, after which this site will then be added to the set $Y$, and a new avalanche might occur. Note that when parallel updating is used, the models become abelian in the updating of active sites, as they are updated "simultaneously". This is not the case when sequential updating is used, as now the order in which active sites are updated, and thus the order in which sites topple, does have an immediate effect on the other active sites. Take for example the set of two active neighbouring sites $\{14, 15\}$. If now site $i = 15$ is designated to topple, it will do so *before* site $i = 14$ is even checked. Site $i = 15$ thus now topples according to the rules in in section (2.1), and in doing so changes the slope $z_{14} = h_{14} - h_{15}$ before this site is checked. Furthermore, site $i = 14$ is now declared as being active twice, which means it will be checked twice in the future. This is not the case in parallel updating, as here the set $Y$ is a set in the mathematical sense, in which all elements are unique. Note that, in sequential updating, it thus doesn't make much sense to speak of the sets $Y$, $X$ and $Y'$.

The order in which topplings occur thus possibly has a big influence on the outcome when sequential updating is used, and one also introduces a certain subjectiveness in this order in which active sites are updated. Although no mention is made in [22] about which method of updating is used, it therefore seemed more natural to use parallel updating instead of sequential updating. However, even though the differences between the models discussed here and those in [22] became considerably smaller when using parallel updating, some unexplainable differences still remain. These differences, however, are of no importance for any of the results presented in this thesis.

# 3 Avalanche dynamics

Since the dynamics of the systems, governed by the rules introduced in section (2), give rise to power-law distributions of avalanches with size $s$, it might be interesting to have a look at how these dynamical rules affect the resulting states, both during and after relaxation. We noticed for example that, in the unlimited models, there is this occurrence of rare, relatively very large, avalanches. Investigation shows that, in the unlimited models, there are also rare occurrences of very steep slopes during relaxation, which is most likely one of the main causes of these rare large avalanches. This observation raised the question of how these steep slopes are formed, which will be elucidated in subsections (3.3.1) and (3.3.2). Furthermore, in the following sections we will take a look at how the dynamics of the avalanches affects the states after relaxation, which is done by investigating if there are any critical properties to be found in this, possibly critical, steady state.

## 3.1 Transient and recurrent states

Let us start with a short explanation of the evolution of our states during a simulation. We start in a state that occupies a point in phase space which either lies in, or very near, the attractor of the dynamics. The states lying within the attractor are stable states by definition, as they result from the dynamics. However, there also exist stable states lying outside the attractor, which are only encountered when the initial state lies outside the attractor. These states are part of the set of transient states $T_i$, which is the set of states that will never be encountered again as a result of the dynamics. The stable states that form the attractor are termed as recurrent states $R_i$, and these states can be encountered again through the dynamics of the systems. Assuming we start in an initial transient state, the recurrent states are then reached by adding a certain required amount of particles to the transient states in between relaxations. The set of recurrent states thus forms the attractor, and when this set is reached, the system will remain there forever. Assuming $k$ depositions of particles are needed to enter the attractor, the evolution of the models can be represented as

$$T_1 \rightarrow ..... \rightarrow T_k \rightarrow R_1 \rightarrow R_2 \rightarrow ....., \tag{3.1.1}$$

where $k$ is minimized by starting as close as possible to the attractor. It is in these recurrent states where our interest lies. Of course, in practise, the steady state we observe is probably only a subset of the set of recurrent states $R_i$. Now, in general, not much can be said about the exact form of the attractor, or about the path that will be traced out within this attractor by the evolution of the system during a simulation. Therefore, not much can be said about the distribution of the recurrent states. In equilibrium physics, the states are distributed according to the well-known Boltzmann distribution, but in models displaying SOC such distributions are not known in general. Still some things can be said about the set of recurrent states. In the following section we will investigate the possible criticality of the steady state in all four models, and in sections (3.2.1) and (3.2.2), bounds on the slopes $z_i$ of the recurrent states are found. Note that these bounds do not necessarily translate directly to bounds on the heights $h_i$, as the

map between the set of recurrent states expressed in "height-space", and expressed in "slope-space", is not necessarily one-to-one. If, however, one makes an attempt to find the distribution of the recurrent states in slope-space, then the bounds on this space might be helpful. Here, height-space and slope-space are used to refer to the phase space of the system in which the states are expressed in terms of heights and slopes respectively.

### 3.1.1 Criticality in the recurrent states?

In the original $2d$ BTW model [1], it was shown that the correlation length and the correlation time diverge in the thermodynamic limit when the system reaches its steady state. Majumdar and Dhar [23], then showed the existence of a height-height correlation function in the general $d$-dimensional ($d \geq 2$) Abelian sandpile model, which decays with distance $r$ between sites as $\sim r^{-2d}$. In addition to the scale-invariant behaviour found in the avalanche-distributions, the steady state itself thus also exhibits scale-invariant properties in the BTW model. These observations might suggest that the avalanche-distributions obeying a power-law do not necessarily emerge solely from the dynamics, but possibly are related to this scale-invariant behaviour exhibited by the variables making up the steady state. Naturally, the question arose as to whether there were also some critical properties to be found in the steady states of our one-dimensional models. In our search for this criticality in the steady states, we look at a few different properties of the recurrent states. First, the roughness in the profile of the slopes $z_i = h_i - h_{i+1}$ of the steady state is measured, which is analysed by looking at two different measures of this roughness in all four models. Secondly, the distribution of slopes $z_i$ is studied in multiple ways. First, the correlation between slopes in all four models is investigated by defining a slope-slope correlation function. Thereafter, to investigate the correlations further, a few distributions are investigated, which are mainly based on the distances between certain slopes taking on equal, or similar values. All these properties will be discussed in the following two subsections. Note that, although the avalanche-distributions emerging in local-unlimited model are not convincing enough to take into consideration, still some critical properties may be found in its steady state. We therefore also include this model into our analysis of the, possibly critical, steady states.

#### 3.1.1.1 Roughness in slopes

The surface profile of the steady states is thus studied by calculating two measures of roughness. Usually, this roughness is studied by looking at the height-profile of the system. Here, however, we measure these quantities by looking at the roughness in slopes as opposed to the roughness in heights. Of course, measuring the roughness in slopes also tells us something about the roughness in the height-profile, but since in at least three of our four models the values of the heights in the steady states always occupy values in descending order from closed to open boundary, measuring the roughness in height-space would therefore probably lead to less precise results. On the other hand, the surface profile in slope-space varies in both directions with respect to some average slope $\bar{z}$ of the state, and expressing our measures of roughness in slope-space might therefore be more suitable. The following two measures of roughness are defined:

$$R = \sum_{i,j=1}^{L} \langle (z_i - z_j)^2 \rangle = \sum_{i,j=1}^{L} \langle ((h_i - h_{i+1}) - (h_j - h_{j+1}))^2 \rangle, \tag{3.1.2}$$

and

$$R^* = \frac{1}{L^2} \sum_{i,j=1}^{L} \langle (h_i - h_j - \bar{z}(i-j))^2 \rangle, \tag{3.1.3}$$

where $\langle \cdot \rangle$ denotes the ensemble average, $\bar{z} = \frac{1}{L}\sum_{i=1}^{L} z_i$ is the average slope in the particular state at hand, and $z_i$ and $h_i$ are the slope, and height, at site $i$ respectively. In Eq.(3.1.2), all the slopes $z_i$ are compared with all other slopes, providing a measure of the deviation between individual slopes with the rest of the profile. The second quantity (3.1.3) can be seen as giving a measure of the deviations of the slope between site $i$ and $j$ as compared to a smooth flat average-slope-profile. Both quantities give zero when there is no roughness, and some non-zero, positive value when any profile deviations in the slopes are measured. We measure the roughness for different system-sizes $L$, and if the steady states of our models display any criticality in their roughness, we expect these quantities to scale with a non-trivial power of this system size $\sim L^{\alpha}$. Here, the roughness exponent $\alpha$ is regarded as non-trivial if its value differs significantly from $\alpha = 2$. When there is no non-trivial growth of roughness, both quantities are expected to grow with $L^2$, since the number of terms just scales quadratically. Both quantities are measured simultaneously, and thus are averaged over the same set of recurrent states for every given $L$. In order to avoid any subjectiveness in the calculations of these quantities, we look at ensembles of recurrent states which are as similar as possible for every given system size $L$. This is done by only considering the states that arise after a certain amount of topplings have occurred during the avalanches. This minimal amount of required topplings is set by hand for the smallest system in consideration, after which the amount grows with a factor proportional to that of the scaling of the largest observed avalanches $\mathrm{s_{max}}$ with system size $L$, as $\mathrm{s_{max}^{new}} \propto (\mathrm{L_{new}}/\mathrm{L_{old}})^{\nu} \cdot \mathrm{s_{max}^{old}}$. Here, $\nu$ is a critical scaling exponent which will be elucidated further in section (4). Furthermore, the sizes of the systems on which the measurements will be performed are $L = 35, ..., 8960$, where every precedent $L$ is multiplied by a factor of 2. The minimal amount of required topplings for our smallest system $L = 35$ is set to $n = 8L$, after which this amount $n$ thus gets multiplied by a factor of $(\mathrm{L_{new}}/\mathrm{L_{old}})^{\nu} = 2^{\nu}$ for every subsequent $L$.

Measurements of the roughness $R^*$ as defined in Eq.(3.1.3) show trivial scaling exponents of system size $L$ in all four cases, meaning scaling exponents $\alpha \approx 2$ were observed in the steady states of all our models. When measuring the roughness $R$ defined in Eq.(3.1.2), similar trivial scaling exponents $\alpha \approx 2$ were again observed in both the limited models. However, in the unlimited models, non-trivial critical scaling exponents arose when measuring the roughness $R$. In Fig.1 the resulting power-law of this roughness as a function of system size $L$ is shown on log-log scale for the local-unlimited model, for which a critical roughness exponent $\alpha = 1.804 \pm 0.001$ is obtained. In Fig.2, the power-law exhibited by the nonlocal-unlimited model is shown, for which the roughness exponent takes on the value $\alpha = 1.628 \pm 0.001$. The power-laws in Fig.1 and Fig.2 indicate a non-trivial growth in the roughness of the steady states of both the local, and nonlocal-unlimited model, and might be indicative of non-trivial slope correlations. Interestingly, this form of criticality thus only seems to arise in the steady states of the unlimited models. Also note that, although no convincing critical behavior was found as arising from the dynamics in the local-unlimited model, there thus does exist at least one critical property intrinsic to the steady state of this model.

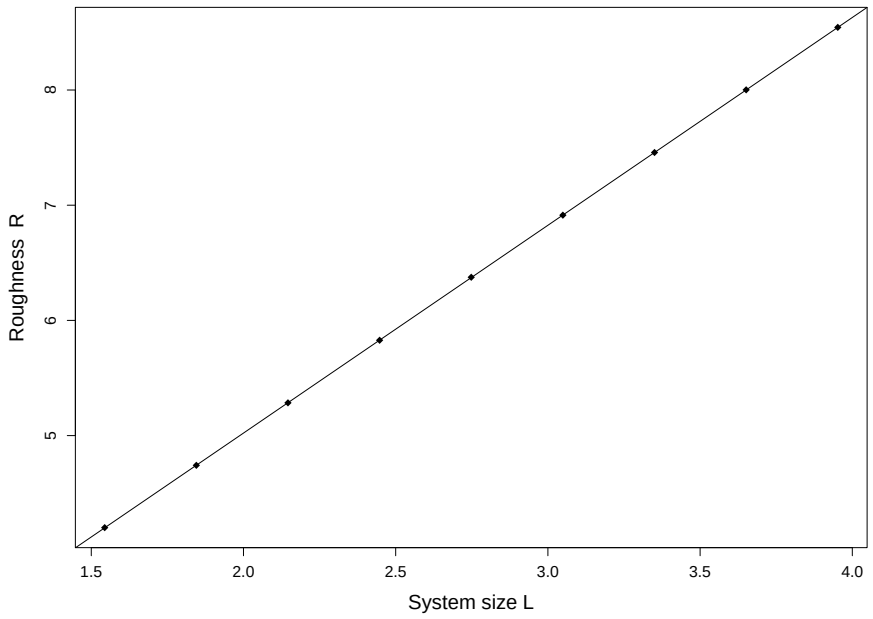


Figure 1: A base 10 log-log plot of the roughness $R$ of the local-unlimited model as defined in Eq.3.1.2. The black dots represent the measured data points. The black line is our fit with slope $\alpha = 1.804 \pm 0.001$. The roughness $R$ thus follows a power-law $\sim L^{\alpha}$ with non-trivial scaling exponent. System sizes $L = 35, ..., 8960$ were used, and the parameter-values were set to $g = 1/8$ and $z_c = 6$ .

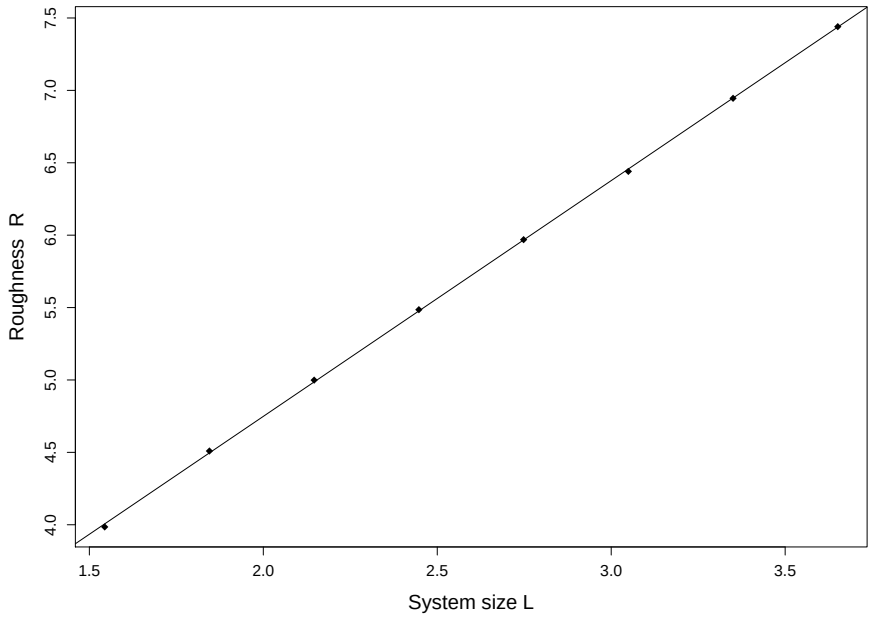


Figure 2: A base 10 log-log plot of the roughness $R$ of the nonlocal-unlimited model as defined in Eq.3.1.2. The black dots represent the measured data points. The black line is our fit with slope $\alpha = 1.628 \pm 0.001$. The roughness $R$ thus follows a power-law $\sim L^{\alpha}$ with non-trivial scaling exponent. System sizes $L = 35, ..., 4480$ were used, and the parameter-values were set to $g = 1/8$ and $z_c = 6$. Note that the system size $L = 8960$ is left out in this case, as the ensemble over which the average is taken turned out to be too small to make any reasonable estimates of the average roughness $R$.

The observant reader might have noticed that the roughness $R^*$ scales as $\sim L^4$ if we do not divide the quantity by $L^2$. This is because, in addition to the number of terms in $R^*$ that grows with a factor of $(\mathrm{L_{new}}/\mathrm{L_{old}})^2$, the terms themselves also, on average, grow with this same factor. This results from the fact that the ensemble average height $\langle \bar{h} \rangle = \langle \frac{1}{L} \sum_{i=1}^{L} h_i \rangle$ of the steady states grows with a factor of $(\mathrm{L_{new}}/\mathrm{L_{old}})$, implying that, on average, the terms in Eq.(3.1.3) will grow with a factor of $(\mathrm{L_{new}}/\mathrm{L_{old}})^2$, resulting in a total growth factor of $(\mathrm{L_{new}}/\mathrm{L_{old}})^4$. This means, if we take $(\mathrm{L_{new}}/\mathrm{L_{old}}) = (mL/L) = m \in \mathbb{Z}^+$ for example, that we can write $\langle \bar{h} \rangle_{mL} \approx m \cdot \langle \bar{h} \rangle_L$, where the subscript now represents the size of the system over which $\langle \bar{h} \rangle$ is calculated. One might expect that this also implies that $\langle h_{mi} \rangle_{mL} \approx m \cdot \langle h_i \rangle_L$, where $\langle h_i \rangle_L$ is the ensemble average of the height at a particular site $i$ for a given system size $L$. This, however, isn't necessarily true for all $i$, as $\langle h_{mL} \rangle_{mL} \approx \langle h_L \rangle_L$ for any given $L$ and $m$ for example. What it rather implies, is $\langle h_{k=mi-m+1,\ldots,mi} \rangle_{mL} = x_k \cdot \langle h_i \rangle_L$, where the average of $x_k$ satisfies $\bar{x} = \frac{1}{mL} \sum_{k=1}^{mL} x_k \approx m$ (here $i = 1, \ldots, L$, and thus $k = 1, \ldots, mL$). This means that in general $\langle h_i \rangle_{mL} > m \cdot \langle h_i \rangle_L$ for $i = 1, \ldots, L$, and, on average, a scaling of $R^* \sim m^4$ is observed. In the local-limited model for example, we see that the value of $x_{k=1}$ starts slightly above $m$, then slowly decreases along the system, after which is plummets near $k = mL$, and takes on the value $x_{mL} \approx 1$ at $k = mL$.

#### 3.1.1.2 Correlations in slope-space

In this section, the correlations between the slopes $z_i$ in the steady state are studied. In second-order phase transitions, the correlation length, defining the length over which the micropic variables are still correlated, diverges when a system approaches its critical point. This divergence gives rise to a correlation function following a power-law as function of the distance between the variables of which the correlation is measured. The critical behaviour found in the roughness of the slope-profile in the two unlimited models might be an indication of such non-trivial correlations between the slope-variables in the steady states of these models. Naturally, this leads us to the question of whether such correlations also can be found in these unlimited steady states. Additionally, although displaying trivial roughness exponents, the slopes in the steady states of the limited models might still be non-trivially correlated, and thus will also be investigated. In order to answer this question, the correlations between the slope-variables $z_i$ and $z_j$, at site $i$ and $j$ respectively, are studied by means of a slope-slope correlation function. To be more precise, we will look at correlations of the fluctuations of $z_i$ and $z_j$ from the average slope $\bar{z}$. These correlations are studied using the following correlation function

$$G(i,j) = \langle (z_i - \bar{z})(z_j - \bar{z}) \rangle, \tag{3.1.4}$$

where again $\langle \cdot \rangle$ is the ensemble average, and $\bar{z} = \frac{1}{L} \sum_{i=1}^{L} z_i$ the average slope of the particular state at hand. Note that, when $\bar{z}$ equals $\langle z_i \rangle$, $\langle z_j \rangle$, we obtain the ordinary covariance $Cov(z_i, z_j) = \langle z_i z_j \rangle - \langle z_i \rangle \langle z_j \rangle$ between the two random variables. In general, however, it seems that $\bar{z} \neq \langle z_{i,j} \rangle$ holds in the majority of the cases, as $\langle z_i \rangle$ slowly varies with $i$, but $\bar{z}$ seems to be rather constant over all states. Just to be sure, both forms, that is $\bar{z} = \langle z_{i,j} \rangle$ and $\bar{z} \neq \langle z_{i,j} \rangle$, are studied. We do this by looking at three distinct cases. First, three sites $i$ are chosen at random. The first site is selected somewhere near the start of the system, the second site somewhere in the middle, and the last site somewhere near the end. Thereafter, the correlations between the

variable $z_i$ at these three sites $i$, and the variables $z_j$ at all other sites $j$, are studied seperately for these three distinct cases. The ensemble average is taken over at least $5 \cdot 10^3$ recurrent states, the amount of topplings $n$ that must have occurred in between measurements on these recurrent states is set to $n = 10L$, and system sizes $L = 600, 1000, 3000$ are considered.

We find that the correlation function defined in Eq.(3.1.4), and the covariance $Cov(z_i, z_j)$, show no significant differences, and both do not seem to exhibit critical behaviour in the correlations in any of the models. In fact, no significant correlations were observed at all, as the resulting data mostly oscillates around zero in all four cases. Although the data seems to display some correlations over certain ranges in some models, no criticality, in the form of a power-law decay with distance $|i - j|$, can be identified in these correlations. Based on these results, one might be inclined to the conclude that no correlations between the slope-variables, and therewith no critical behaviour in these correlations, can be found in the steady states in any of our models. However, since the data is very noisy, and therefore not very convincing, we will study the possible existence of correlations further by looking at certain distributions of the slopes. In particular, we look at the distribution of the occurrences of distances $|i - j|$ between the slope-variables $z_i = c$ and $z_j = c$. We start by looking at the distribution of all distances between $z_i = 13$ and the *next nearest* $z_j = 13$ in a given state. The value $z_i = 13$ is chosen because, according to Eq.2.1.1, this is the highest possible slope-value in all steady states (given our values $g = 1/8$ and $z_c = 6$). This distribution is calculated by iterating over all values $i$ in a given state. If then a slope $z_i = 13$ is encountered, the distance to the next nearest slope $z_j = 13$ is saved, afterwhich $i$ becomes $j$ and the process repeats itself until the end of the system is reached. In both the local, and nonlocal-limited model, the outcoming data suggests that the occurrences of these distances between $z_i = 13$ and $z_j = 13$ follow an exponential distribution, that is, the random variable $|i-j|$ is exponentially distributed. From this observation, we can conclude that the occurrence of the slope-variables taking on $z_i = 13$, is poisson distributed along the system, and that these events thus occur randomly and independently. Moreover, further investigation shows that the distance $|i - j|$ follows an exponential distribution for all possible slope-values $z_i$ in both the limited models. In Fig.3, the occurrences $P(|i - j|)$ of distances $|i - j|$ are shown for the local-limited model, where the slope-values are set to $z_i = 7, 9, 11, 13$. Similar distributions were observed in the nonlocal-limited model. We consider these distributions convincing enough to indeed conclude that the occurrences of the slope-variables $z_i$ taking on equal values are poisson distributed along the system, and that these events thus occur randomly and independently. This implies that no correlations exists between the slope-variables in both the limited models, and strongly suggests that the steady states do not need to exhibit any scale-invariance in order to observe some scale-invariant behaviour in the form of avalanche-distributions following a power-law. It thus seems that these distributions emerge solely from the dynamics in the limited models, and do not require any critical properties intrinsic to the steady states. In the unlimited models, however, the distances between the slope-variables do not seem to follow an exponential distribution. In fact, we were not able to identify any concrete distributions of distances between slope-variables taking on equal values for any given slope-value. In a last attempt to infer something useful about correlations between slope-variables, we therefore looked at distributions of distances between slope-variables taking on slope-values $z_i > c$, where $c \in \{9, 10, 11\}$ for example. This, however, did not lead to significant differences in the shape of the observed

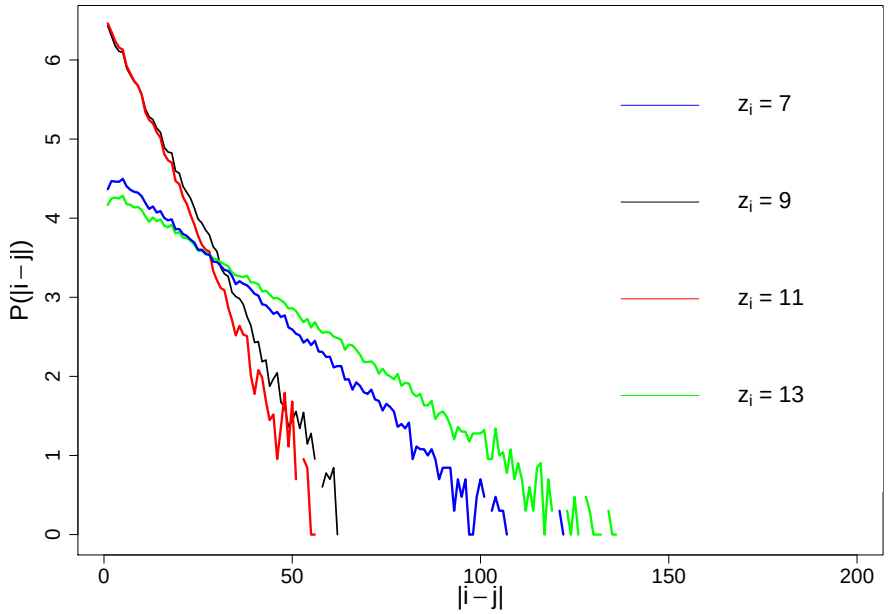


Figure 3: The occurrences $P(|i-j|)$ of distances $|i-j|$ plotted on base 10 semi-log scale for four different values of the slope-variables $z_i$. The distributions are calculated for $L = 200$, $N_0 = 2$, $g = 1/8$ and $z_c = 6$. The relatively straight lines indicate that the distances $|i-j|$ between slope-variables taking on equal values follow exponential distributions for the given values $z_i = 7, 9, 11, 13$. Similar exponential distributions were observed for all other possible slope-values in both the limited models.

distributions, and thus did not provide any useful additional information. The possible existence of non-trivial correlations, and therewith a possible connection between the steady states and the critical avalanche-distributions (or lack thereof in the local-unlimited case), therefore remains unknown in these models, and further investigation is needed to make decisive conclusions on this matter.

### 3.2 Limitations on slopes

As mentioned above, the precise form of the attractor, and the distributions of recurrent states, are not known in our one-dimensional SOC models. Still, some things can be said about the attractor and these distributions by providing lower, and upper-bound on the slopes occurring in the recurrent states. In this section, we will try to find lower, and upper-bounds on the slopes of the recurrent states, providing bounds on the slope-space, and therewith also on the attractor of the dynamics and the distributions of these recurrent states. Additionally, we provide estimates of the upper-bounds on the slopes in the states of the unlimited models during relaxation. Interestingly, the upper-bound on the slopes, and therewith the maximum number of particles that drop in a single toppling event, scales as $\sim L^{\zeta}$ in the nonlcocal-unlimited model, whereas in the local-unlimited model, is only grows very slightly with $L$, and no concrete relation is found.

### 3.2.1 Lower-bounds on slopes

We will start by providing lower-bounds on the recurrent states of the limited models. Imagine the following situation in the slope-space of the local-limited model, in which all sites occupying a slope-value $z_i > z_c = 6$ will topple $N_0 = 2$ particles to their right-neighbour

$$7, 6, 7, 5, 8, 6 \;\rightarrow\; 3, 10, 3, 9, 4, 8. \tag{3.2.1}$$

Since $z_i = 7$ is the minimum required value in order for a site to topple with some non-zero probability, we can see that a minimum slope-value of $z_{min} = 3$ is obtained in the case of $z_c = 6$ and $N_0 = 2$. With some calculations, the general expression $z_{min} = z_c - (2N_0 - 1)$ can be found for the local-limited model. For the nonlocal-limited model, we can imagine the following situation in slope-space, in which again all sites occupying a slope-value $z_i > z_c = 6$ will topple $N_0 = 2$ particles to their right-neighbours

$$7, 6, 7, 5, 8, 6 \;\rightarrow\; 4, 8, 5, 6, 5, 7. \tag{3.2.2}$$

Since $z_i = 7$ is the minimum required value in order for a site to topple with some non-zero probability, we can see that a mimum slope-value of $z_{min} = 4$ is obtained in the case of $z_c = 6$ and $N_0 = 2$ for nonlocal-limited model. With some calculations, the general expression $z_{min} = z_c - (2N_0 - N_0)$ can be found for the nonlocal-limited model. For the nonlocal-unlimited model, we can imagine the following situation in slope-space, in which again all sites occupying a slope-value $z_i > z_c = 6$ will topple, but now $N = z_i - z_c$ particles will fall to their right-neighbours

$$7, 6, 7, 6, 7, 6 \;\rightarrow\; 5, 8, 5, 8, 5, 7. \tag{3.2.3}$$

Of course this is a very unlikely situation to occur, but it serves its purpose, and since again $z_i = 7$ is the minimum required value in order for a site to topple with some non-zero probability, we can see that a mimum slope-value of $z_{min} = 5$ is obtained in the case of $z_c = 6$. In this case, we immediately can deduce the general expression $z_{min} = z_c - 1$ for the nonlocal-unlimited model. A lower-bound on the slopes in the local-unlimited model is, however, harder to obtain. This results from the fact that, during avalanches, very steep slopes can be formed in this model, which will be elucidated further in section (3.3). These steep slopes of course topple with certainty, but in the local-unlimited model, they can leave behind large negative slopes, which can remain until after relaxation. However, since the steep slopes in the local-unlimited model seem to grow very slowly with $L$, one might expect that the slope-space is thus also somewhat bounded from below. Simulations indeed show, a relatively constant minimum slope $z_{min} \approx -28$, which doesn't seem to grow with system size. If this behaviour holds in the thermodynamic limit is unknown. Note that, at least in both the limited models and the nonlocal-unlimited model, the lower-bounds apply both to the recurrent states and the states during relaxation. This is not true for the upper-bounds, which will be given in the following section.

### 3.2.2 Upper-bounds on slopes

In this section, in addition to the upper-bound on the slopes of the recurrent states in all four models, also the upper-bound on the slopes of the states during relaxation of both the local, and nonlocal-unlimited model will be investigated. Of course, the maximum value $z_{max}$ of the

allowed slopes in the recurrent states of all four models is easily found, as $z_{max} = z_c + (1/g - 1)$, where $g$ is the parameter introduced in section (2). The upper-bounds on the slopes of the states occurring during relaxation of the limited models isn't necessarily interesting, as the slopes in these models do not exceed the maximum slope $z_{max}$ of the recurrent states by much. In the unlimited models, however, we noticed the forming of very steep slopes during relaxation, of which the forming will be elucidated further in the following sections. For now, we will focus on the question of how, and if, these steep slopes scale with system size $L$. Remarkably, for the nonlocal-unlimited model we obtain a scaling of these steep slopes $z^*$ of the form $z^* \sim L^{\zeta}$, where $\zeta = 0.354 \pm 0.001$.

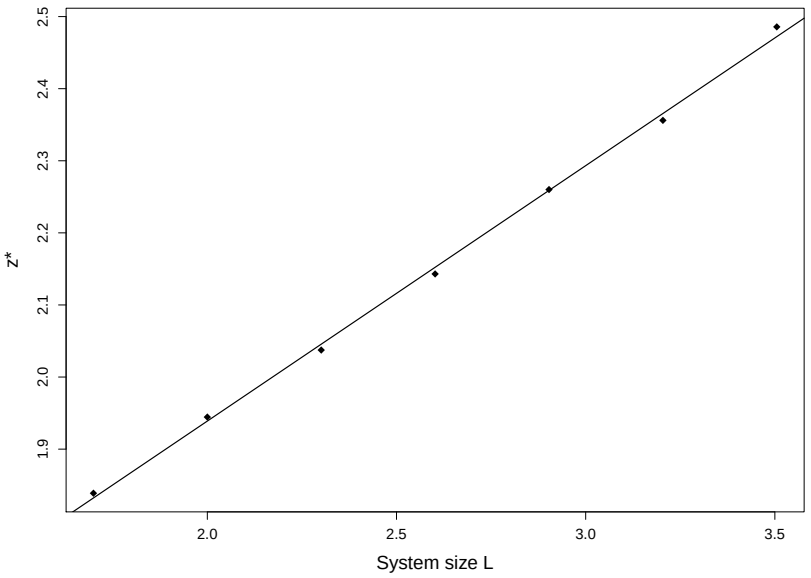


Figure 4: A base 10 log-log plot of the steepest observed slope $z^*$ in the states occurring during relaxation in the nonlocal-unlimited model. The black dots represent the measured data points. The black line is our fit with slope $\zeta = 0.354 \pm 0.001$.

In Fig.4, the obtained power-law is displayed for system sizes $L = 50, 100, 200, 400, 800, 1600, 3200$. Contrary to the nonlocal case, no scaling was observed in the local-unlimited model. The steep slopes $z^*$ do grow slightly, but very slowly, with $L$, and no clear relation seems to exist. The slopes in the states occurring during relaxation of the nonlocal-unlimited model are thus unbounded in the thermodynamic limit, whereas no conclusion can be drawn on the upper-bound of the slopes in the local-unlimited model. Although investigating these upper-bounds doesn't tell us anything about the attractor of the dynamics per se, it still gave rise to interesting behaviour. On the other hand, the upper, and lower-bounds on the slopes of the recurrent states do provide us with bounds on slope-space, and therewith with bounds on the attractor. With the information provided by these bounds, in combination with the distributions found in section (3.1.1.2), the ensemble average of the slopes $\langle z_i \rangle$ and ensemble average of the average slope $\langle \bar{z} \rangle$, one could try to find a distribution, analogous to the boltzmann distribution in equilibrium physics, of these recurrent states. One could, for example, try to find this distribution by defining a recurrent state according to some scalar measure of slope-units ($\sim \sum_{i=1}^{L} z_i$), where then certain states are more likely to occur than others according this measure.

### 3.3 Formation mechanisms of steep slopes

In the following two subsections, we turn to the states that occur during relaxation. Amaral et al. [22], mention that no differences between the critical avalanche exponents arise when defining the avalanche-size $s$ as the total potential energy dissipated in between avalanches [9], or as the total number of topplings ($\mathrm{s_{top}}$) that occur during relaxation. Their explanation is that, on average, a fixed amount of potential energy is dissipated per toppling event, meaning that the distribution just should shrink, or stretch , when switching between both definitions. This would also imply that no differences in the exponents should arise when we define the $s$ as the total number of particles that drop during relaxation ($\mathrm{s_{drop}}$) versus $\mathrm{s_{top}}$, since, on average, a fixed amount of particles should drop in a single toppling event. Of course, this holds true for both the limited models, as the number of particles that drop in one toppling event is $N_0$. However, in the unlimited models, we do observe a change in the exponents when using the definitions $\mathrm{s_{top}}$ versus $\mathrm{s_{drop}}$ for avalanche-size. One might wonder how the exponent of the local-unlimited model can change when no well-behaved power-law of $\mathrm{s_{top}}$ is observed in this model. Surely, we cannot speak about a change in exponents for this model, but the local-unlimited model does seem to display semi power-law behaviour when $\mathrm{s_{drop}}$ is used as the definition of avalanche-size. The emphasis here lies on semi, as, although a straight line is observed on a log-log scale, the scaling of this straight line stops at system sizes $L > 1500$. In trying to explain the differences between the distributions of $\mathrm{s_{top}}$ and $\mathrm{s_{drop}}$, the distributions of the number of particles that drop in a single toppling event, calculated over all avalanches, were plotted. The distributions that arose, were exponential distributions for both the unlimited models, in which the number of particles that drop in one toppling event ranged from 1 to around 100 for $L = 200$, and this range thus grows in accordance with the growth of steep slopes with system-size as explained in section (3.2.2). These exponential distributions will be shown in section (3.3.3). However, these distributions seem to confirm that, on average, a fixed amount of particles should drop in a single toppling event, since an exponential distribution has a well-defined average. It thus seems like there exists an inconsistency between the exponential distributions of particles dropping in a single toppling event, and the observation that the exponents of the avalanche distibutions have a different value when considering $\mathrm{s_{top}}$ versus $\mathrm{s_{drop}}$. To check whether there indeed exists such an inconsistency, some explicit calculations will be performed in section (6.1.1). For now, we focus on another interesting feature that can be inferred from the exponential distributions, namely the occurence of very steep slopes, as a large number of particles dropping in a single toppling event requires a difference in heights $z_i = h_i - h_{i+1}$ equal the number of particles that drop in one toppling, plus the critical slope $z_c$. This is an interesting feature because, firstly, it might not be so obvious how these steep slopes can build up, and secondly, very large outliers were observed in the avalanche-data of the unlimited models, for which these large particle-drops per toppling might serve as an explanation. Also, in the recurrent states, the maximum allowed slope is $z_i = 13$ according to Eq.(2.1.1) when setting $z_c = 6$. This is because the probability $p(z_i)$ with which the site $i$ topples becomes 1 when the slope exceeds $z_i = 13$. One can imagine that this maximum value of $z_i$ might be slightly exceeded during relaxation, but the amount by which this value is exceeded in the unlimited models was not expected, and this raised the question of how these very steep slopes are formed.

### 3.3.1 The nonlocal-unlimited case

We will start by investigating the forming of very steep slopes in the nonlocal-unlimited model. This is done by observing an ensemble of states that occur during an avalanche in which a large number of particles falls in a single toppling event. These states are expressed in terms of slopes, from which the mechanism behind the forming of very steep slopes is inferred just by observation. Note that we thus define a slope $z_i$ to be steep when it at least exceeds $z_i > z_c + (1/g - 1) = 13$ in this particular case. The first thing we note, is that very steep slopes often are accompanied by multiple other steep slopes, and thus rarely occur alone. Careful observation of these states in which multiple steep slopes occur, lead us to the following explanation of the forming of steep slopes. According to Eq.(2.1.1), slopes of $z_i = 13$ are thus allowed when $z_c$ is set to 6. Now, it is always possible that this site receives a particle from one of its left neighbours in accordance with the toppling rules in Eq. (2.1.3). The slope at site $i$ will now take on the value $z_i = 14$ in the nonlocal-unlimited case, and $z_i - z_c = 8$ particles are guaranteed to fall from site $i$ to site $i+j$, where $j = 1, ..., 8$. There exists, however, a probability that, although the height $h_i$ exceeds the height $h_{i+1}$ by 14, the height $h_{i-1}$ exceeds the height $h_i$ by 13 for example. This results from the fact that we always add a particle at the most left site $i = 1$ in between avalanches, which causes a state in which the heights are build up in descending order from closed to open boundary in our models. When site $i$ then topples, we can represent the change in slopes at sites $i - 1$ and $i$ in the following way

$$13, 14 \;\rightarrow\; 21, 5, \tag{3.3.1}$$

where the resulting situation of slopes is thus $21, 5$ after site $i$ topples $z_i - z_c = 8$ particles to its 8 right-neighbours. Now the difference between $h_{i-1}$ and $h_i$ is 21, and site $i - 1$ is thus, with certainty, going to topple $z_i - z_c = 15$ particles to its 15 right-neighbours. But since the height-profile is in descending order from closed to open boundary, one can imagine that the height at site $i - 2$ exceeds the height at site $i - 1$ by 12 for example. When site $i - 1$ then topples, we can represent the change in slopes at sites $i - 2$ and $i - 1$ in the following way

$$12, 21 \;\rightarrow\; 27, 5, \tag{3.3.2}$$

after which site $i - 2$ will topple $z_i - z_c = 21$ particles to its 21 right-neighbours with certainty. There thus exists some building-up mechanism, in which a steep slope is formed from open to closed boundary. This mechanism can start at any random site, and the formed slope can evolve from this site all the way up to the closed boundary. Note that the slope at site $i$ only grows when the left-adjacent slope $i-1$ exceeds $z_c$, which, on average, is the case, as $\bar{z}$ slightly exceeds $z_c$ in this model. One can imagine that, when this building-up mechanism starts near the open boundary at the right, very steep slopes, although exponentially unlikely, can be formed. Since there exists a building-up mechanism evolving from closed to open boundary, with a little imagination one can make the link to nature by thinking of an iceberg in Antarctica for example. This iceberg initially has a relatively constant slope, after which two slanted plateaux are slowly formed near the edge. These plateaux are separated by the slowly growing steep slope when evolving from the cliff of the iceberg to the centre, and in doing so, ice crumbles down, falling from the higher to the lower plateau, resembling avalanches of ice, of which part gets lost at the edge and falls into the sea. Of course, the observation that very steep slopes often are accompanied by multiple

other relatively steep slopes just translates to multiple plateaux instead of two on the iceberg. As mentioned above, the nonlocal-unlimited model also displays large outliers in its avalanches, which are not seen in the limited models. These occurrences of multiple steep slopes might form a good explanation of these rare large avalanches, as, in addition to the number of topplings needed to form these steep slopes, the large number of particles that fall during these topplings have a large number of active sites as a result, which in turn again may lead to a large number of topplings. This remains, however, speculation, as it is not investigated thoroughly enough to make these statements conclusive.

### 3.3.2 The local-unlimited case

The investigation of the forming of steep slopes in the local-unlimited model will again be done by careful observation of an ensemble of states that occur during an avalanche in which a large number of particles falls in a single toppling event. In this model, the direction in which the forming of steep slopes takes place seems to be opposite to that of the nonlocal-unlimited model, that is, from closed to open boundary. Imagine a slope $z_i = 11$ for example at some random site $i$. According to Eq.(2.1.1), this site topples with a probability $p(z_i) = 5/8$ for $g = 1/8$ and $z_c = 6$, and when it does, it drops 5 particles to its right-neighbour $i + 1$. The probability that the slope $z_{i+1}$ now also exceeds $z_c$ is considerable, as the average slope $\bar{z}$ again slightly exceeds $z_c$. Let us take $z_{i+1} = 13$, which thus still doesn't topple with certainty, but with a probability $p(z_{i+1}) = 7/8$, after which 7 particles will be transferred from $h_{i+1}$ to $h_{i+2}$. The slope at site $i + 2$ will now very likely take on a value $z_{i+2} \geq 14$, and thus will topple with certainty. If site $i$ lies somewhere near the closed boundary, this slope will grow slowly when evolving from left to right along the system, and can become very steep near the end of the pile. Note that, when a site $i$ topples, all particles get transferred to its right-neighbour $i + 1$ according to the rules in Eq. 2.1.3. This is the reason for the occurrence of negative slopes in the recurrent states of the local-unlimited model, as the height $h_{i+1}$ exceeds the height $h_i$ if more than $z_c$ particles got transferred from $h_i$ to $h_{i+1}$ in a single toppling. Again, there thus exists some building-up mechanism of slopes, but now from closed to open boundary. Likewise, with a little imagination, this mechanism behing the forming of steep slopes in the local-unlimited model can be seen as resembling some natural phenomenon. In this case, we can think of a real avalanche, as seen in the snowy mountains. Here, the steep slope can be seen as the avalanche front, which evolves by rolling down the mountain, gaining height in the process. The negative slopes occuring behind the steep slope can also be seen in real life, as the snow in the front of an avalanche tends to be "pushed up" by the snow right behind it. The relatively large avalanche-outliers observed in this model might again be explained by the process of forming multiple very steep slopes during relaxation, but we do not have enough evidence to back such statements up.

### 3.3.3 Exponential particle-drop distributions

As mentioned above, the distributions of the frequency of occurrences of topplings in which $d'$ particles fall, calculated over all avalanches, seem to follow exponential distributions. These distributions $P(d')$, of the number of particles $d'$ that drop in a single toppling event, calculated over all avalanches, are represented in this section. In Fig.5, this distribution is shown for the nonlocal-unlimited model, and in Fig.6, the distribution of the local-unlimited model is shown.

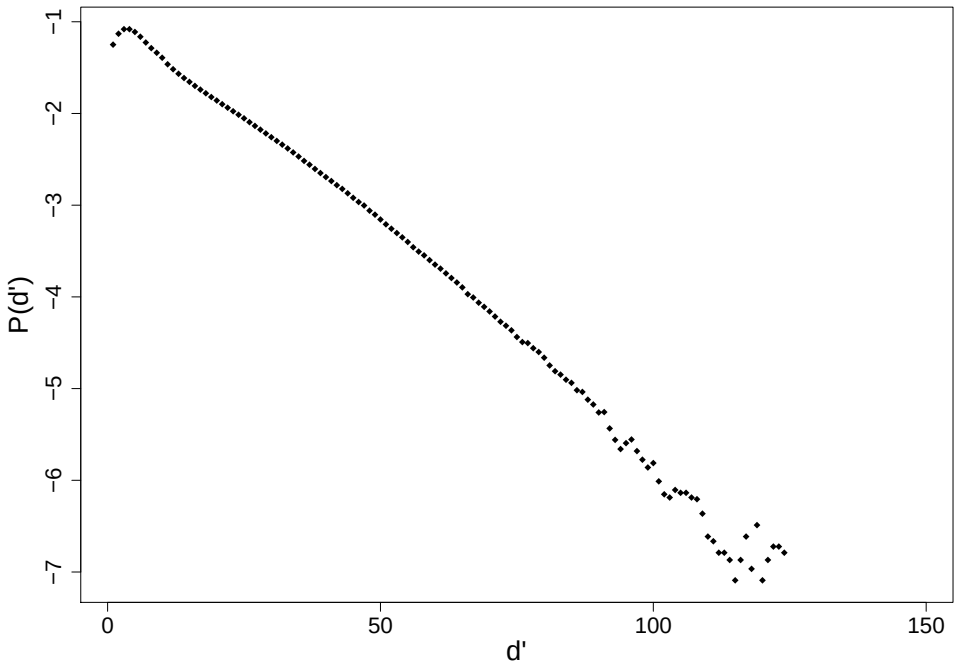


Figure 5: The exponential distribution $P(d')$ of the number of particles $d'$ that drop in a single toppling event, calculated over all avalanches $s > 0$, plotted in semi-log scale for the nonlocal-unlimited model. The system-size used is $L = 200$, and the parameter-values used are $g = 1/8$ and $z_c = 6$.

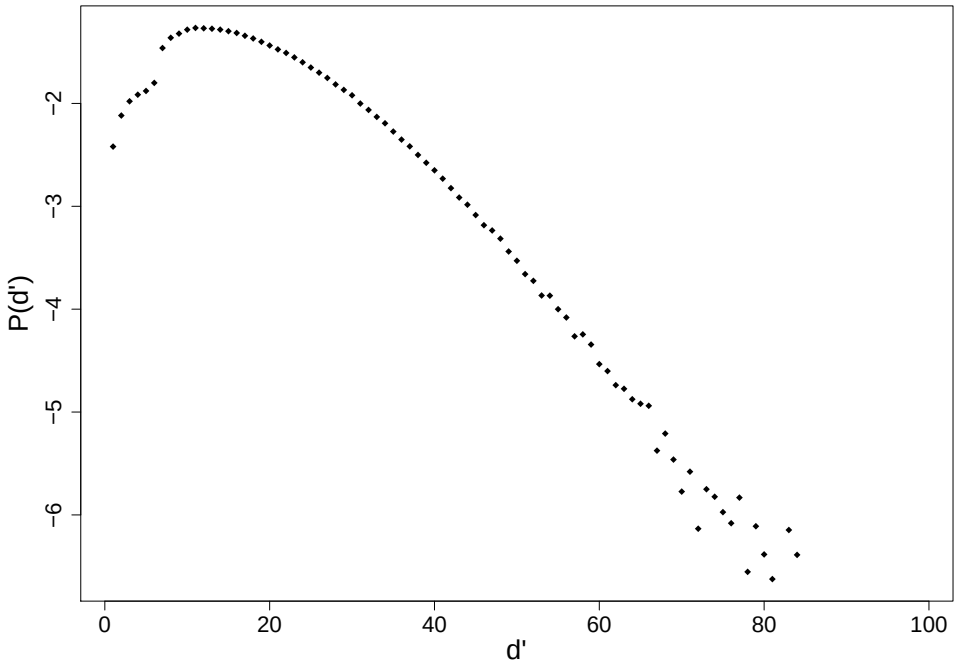


Figure 6: The exponential distribution $P(d')$ of the number of particles $d'$ that drop in a single toppling event, calculated over all avalanches $s > 0$, plotted in semi-log scale for the local-unlimited model. The system-size used is $L = 200$, and the parameter-values used are $g = 1/8$ and $z_c = 6$.

The relatively straight lines observed when plotting the distributions on semi-log scale indicate that the data approximately follows an exponential distribution. We test this by fitting a line through the data, after which we determine the slope of this line, and derive the average amount $\langle d' \rangle$ of particles dropped in a single toppling event during all avalanches from this slope by assuming the distribution is an exponential one. We then calculate the average $\langle d' \rangle$ explicitely by doing simulations, and compare values. Indeed, for the nonlocal-unlimited model we find that these averages are in good agreement, confirming the data approximately follows an exponential distribution. The averages found for the local-unlimited model differ a little more, but are still in reasonable agreement, leading us to believe that the distribution, at least for $d' > 20$ , also approximately is an exponential one. As mentioned above, these exponential distributions seem to be inconsistent with the observation that the avalanche-exponents differ when the avalanche-size is defined as the total number of topplings during relaxation versus the total number of particles that fall during relaxation. Whether there indeed exists such an inconsistency between these, seemingly contradicting, features will be elucidated further in section (6.1).

# 4 Finite-size scaling and critical exponents

In this section, the methods that are used to analyze the critical behaviour emerging from the avalanche-distributions in our models will be discussed, and the results will be presented. Of course, critical behaviour must be characterized by some set of critical exponents. In this analysis, we will make use of the finite-size scaling ansatz, which allows us to extract two critical exponents from our data per definition of avalanche-size, and will be formally introduced in the next subsection. These critical exponents can then be used to characterize the critical behaviour emerging through the dynamics of our models. The first exponent describes how the avalanches of size $s$ are distributed, and the second exponent describes how this distribution depends on system size $L$, that is, how the large avalanches, and therewith the cutoff of the distribution, scale with $L$. The first exponent is calculated with the so-called method of least squares, whereas the second exponent is determined with the help of some analytical derivations in combination with some explicit calculations. Thereafter, to check whether the data is indeed well-described by the finite-size scaling ansatz, and to check whether the calculated exponents are correct, we collapse the data by assuming our data is well-described by this finite-size scaling ansatz. When a proper data-collapse is then obtained, we know the data is well-described by this ansatz, and the critical exponents provide a good description of the behaviour emerging from the dynamics of our models. Furthermore, scale invariance is directly established by a proper data-collapse, implying that we can assume that the behaviour of the distributions holds in the thermodynamic limit, and thus indeed really is critical.

## 4.1 The finite-size scaling ansatz

Strictly speaking, phase transitions, and therewith critical behaviour, only occur in the thermodynamic limit. However, all our simulations are done on systems of finite size, and we therefore want to know how this finite size affects the observed distributions, and if the behaviour we see also holds in the thermodynamic limit. This is where the finite-size scaling ansatz comes in, which is an ansatz used to model the distributions and to investigate the finite size effects of our systems. In using this ansatz, we assume our distributions are well- described by the following power-law form

$$P(s, L) = s^{-\tau} f(s/L^{\nu}), \tag{4.1.1}$$

where $\tau$ and $\nu$ are critical exponents, and $f(s/L^{\nu})$ is some unknown scaling function which describes the finite-size correction to the power-laws. However, because of noise, running-time, and subjectiveness in the representation of binned data, we choose to analyze our data with the use of the integrated, or cumulative, distribution $P(s, L) = Pr(S \geq s, L)$ of Eq.(4.1.1), that is

$$P(s, L) = Pr(S \geq s, L) = \int_s^{\infty} P(S, L) dS = \int_s^{\infty} S^{-\tau} f(S/L^{\nu}) dS = s^{-\delta} G(s/L^{\nu}) \tag{4.1.2}$$

where $s > 0$, $Pr(S > s, L)$ the probability of observing an avalanche $S$ greater than or equal to $s$, $G(s/L^{\nu})$ is again some unknown scaling function and $\delta = \tau - 1$. When making the ansatz in Eq.(4.1.2), we thus expect the distributions $P(s, L)$ of our models to follow a power-law of

avalanche-size $s$ up to some cutoff, which results from the finiteness of the system. This implies there doesn't exist a typical size of avalanches, as the avalanches happen over all size-scales up to the cutoff. These cutoffs, however, do have a typical size, namely $s \approx \alpha L^{\nu}$, where $\alpha$ is some, model-dependent, constant. Indeed, this assures that, as required, no cutoff should be present in the thermodynamic limit $L \to \infty$. The behaviour of the cutoff is modelled by the scaling function $G(s/L^{\mu})$. This implies that this scaling function must take on a constant value for $(s/L^{\mu}) << \alpha$, and is a rapidly decaying function for $(s/L^{\nu}) \geq \alpha$. In the local limited model for example, this rapidly decaying function seems to decay exponentially fast, as we observe a straight line, starting at the cutoff, when plotting the distribution on semi-log scale. As mentioned above, the first exponent $\delta$ is calculated directly with the method of least squares, described in section (4.2.1). In order to obtain the second exponent $\nu$, we first calculate how the average avalanche-size $\langle s \rangle \sim L^{\eta}$ scales with system size $L$. Then we use the following form of this average avalanche-size

$$\langle s \rangle = \int_{s_{min}}^{\infty} sP(s,L)ds = \int_{s_{min}}^{\infty} s^{-\tau+1} f(s/L^{\nu})ds = L^{2\nu-\tau\nu} \int_{x_{min}}^{\infty} x^{-\tau+1} f(x)dx \sim L^{\nu(2-\tau)} \quad (4.1.3)$$

where $x = s/L^{\nu}$, and the integral is assumed to converge for $L >> 1$. Using Eq.(4.1.3) in combination with the calculated exponent $\eta$ in $\langle s \rangle \sim L^{\eta}$, we get $\eta = \nu(2-\tau)$, where $\tau = \delta + 1$ and hence $\nu = \eta/(1-\delta)$. This exponent relation will be used to obtain estimates of the finite-size scaling exponent $\nu$. We obtain $\eta = 1 \pm 0.01$ for both the local, and nonlocal-limited model , and $\eta = 0.32 \pm 0.02$ for the nonlocal-unlimited model. In the next section, we will use these values of $\eta$ to obtain the estimates of the critical exponents $\nu$. Further estimates of $\nu$ can be obtained by using $\langle s^2 \rangle$. What we see, is that these estimates of $\nu$ provide good data-collapses in all cases, and we will use the range around the estimated value of $\nu$ for which these data-collapses remain satisfactory as the error of this exponent.

### 4.1.1 Starting points and cutoffs

As mentioned above, there arises a cutoff in our power-law distributions, which results from the finiteness of the system-size. Additionally, the distributions only seem to follow a proper power-law for avalanches of size $s >> 1$ in most cases. Both these starting points and cutoffs have to be taken into account when calculating the avalanche-exponents of the power-law distributions. To make sure the calculation of these exponents is done over the correct range of avalanche-sizes $s$, we first make an estimate of this range by looking at the plots of the data for each model. Thereafter, this estimated range is divided into $m$ bins of size $n = 10, 25, 50, 100, 500$ data points, after which the exponent is calculated for every single bin of size $n$, thus resulting in $m$ exponents. These exponents are then plotted with respect to avalanche-size, and based on this plot, an estimate is made of the total range over which the exponent must be calculated by observing over which range the $m$ exponents remain relatively constant. The exponents of avalanche-size are then calculated over these ranges for sufficiently large system sizes up to $L = 3200$. This method provides us with good fits in all cases, which is confirmed by the relatively straight constant line observed when plotting the scaling function $G(s/L^{\nu})$ versus $s/L^{\nu}$.

## 4.2 The exponents

When the appropriate range is determined with the method discussed above, the exponents $\delta$ are calculated over this range with the use of the least squares method. Thereafter, the exponents $\nu$ in Eq.(4.1.2) are determined by using the exponent relation $\nu = \eta/(1-\delta)$ derived in section (4.1).

### 4.2.1 Least squares method

The method of least squares, in particular that of linear least squares, is a method in regression analysis that provides us with a straight line fit $y = ax + b$ through the set of $n$ data points $(x_i, y_i)$. In our case, $x_i = \log_{10}(s_i)$ and $y_i = log_{10}(P(s_i, L))$, and thus $a = \delta$. The best fit is obtained by finding the line which minimizes the sum of the squares of the distances $d_i$ between the measured values $y_i = log_{10}(P(s_i, L))$ and this fit $y = \delta x + b$. With some derivations, it can be shown that the exponent $\delta$ is given by

$$\delta = \frac{\sum_i (x_i - \bar{x})(y_i - \bar{y})}{\sum_i (x_i - \bar{x})^2}, \tag{4.2.1}$$

and the offset $b$ by

$$b = \bar{y} - \delta \bar{x}, \tag{4.2.2}$$

where $\bar{x} = 1/n \sum_i x_i$, and $\bar{y} = 1/n \sum_i y_i$ . Furthermore, the error $\epsilon$ in our exponent $\delta$ is given by

$$\epsilon = \sum_i (y_i - \hat{y}_i)^2 = \sum_i (y_i - \delta x_i - b)^2, \tag{4.2.3}$$

where $y_i = log_{10}(P(s_i, L))$ is our raw data, and $\hat{y}_i = \delta x_i + b$ are the corresponding data points on our fit $y = \delta x + b$. Note that all exponents in section (3) were calculated with the method of least squares as well.

### 4.2.2 Exponents based on number of topplings

In this section, we present the critical exponents that are obtained when we define the avalanche-size as the total number of topplings during relaxation, and display the plots and data-collapses of our distributions for all three models. Since the simulations were done for various parameter-values of $g$, $N_0$ and $z_c$, all within the ranges mentioned in section (2.2), we pick randomly chosen values of these parameters for our plots. Furthermore, we denote the total number of topplings $\mathrm{s_{top}}$ occurring during relaxation as $s$ for simplicity.

In Fig. 7, the distributions $P(s, L)$ of avalanches-size $s$ are plotted for the local-limited model. We obtain an avalanche-size exponent $\delta = 0.55 \pm 0.02$ for this model. In Fig. 8, we collapse the data of these distributions onto the function $G(s/L^{\nu})$ by plotting $P(s, L)/s^{-\delta}$ versus $s/L^{\nu}$, where the finite-size scaling exponent $\nu = 2.22 \pm 0.03$ is used.

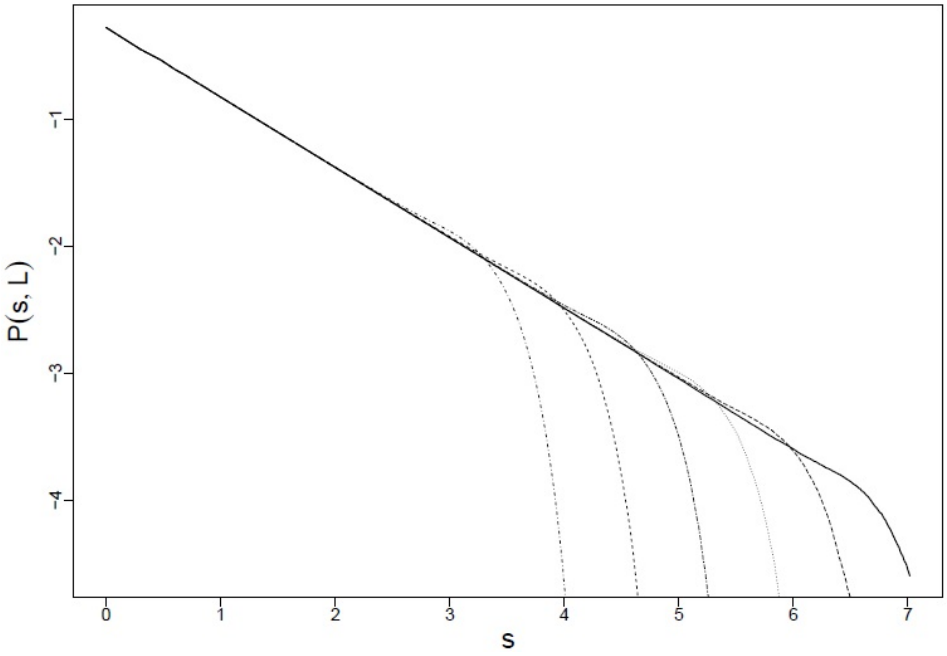


Figure 7: A base 10 log-log plot of the cumulative avalanche-size distributions $P(s, L)$ of the local-limited model for system sizes L = 50,100,200,400,800,1600. The distributions follow a power-law $s^{-\delta}$ for $s >> 1$ up to some cutoff, with critical avalanche-exponent $\delta = 0.55 \pm 0.02$. The parameter-values used are $N_0 = 1$, $g = 1/4$ and $z_c = 1$.

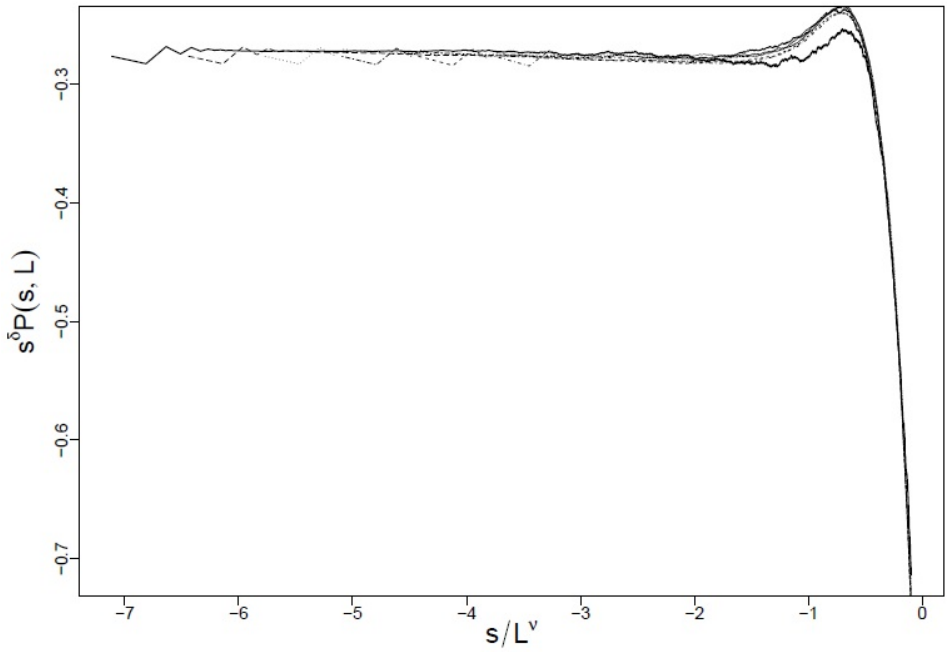


Figure 8: A data collapse of the distributions shown in Fig.7. The data collapse is obtained by plotting the rescaled avalanche-size density $s^{\delta}P(s, L)$ versus the rescaled avalanche size $s/L^{\nu}$, where $\delta = 0.55 \pm 0.02$ and $\nu = 2.22 \pm 0.03$.

In Fig. 9, the distributions $P(s, L)$ of avalanches-size $s$ are plotted for the nonlocal-limited model. We obtain an avalanche-size exponent $\delta = 0.35 \pm 0.05$ for this model. In Fig. 10, we collapse the data of these distributions by plotting $P(s, L)/s^{-\delta}$ versus $s/L^{\nu}$, where the finite-size scaling exponent $\nu = 1.54 \pm 0.03$ is used.

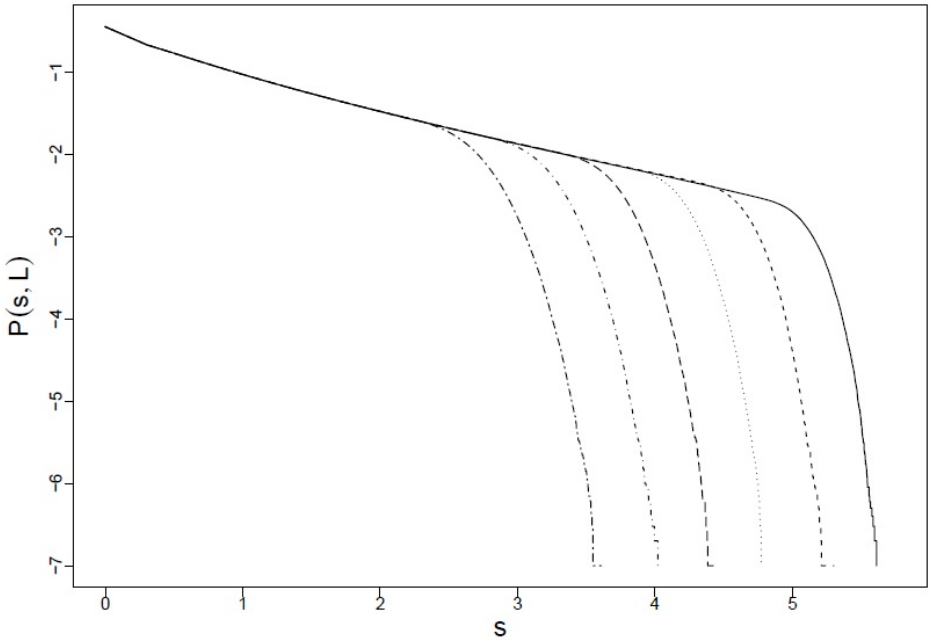


Figure 9: A base 10 log-log plot of the cumulative avalanche-size distributions $P(s, L)$ of the nonlocal-limited model for system sizes L = 50,100,200,400,800,1600. The distributions follow a power-law $s^{-\delta}$ for $s >> 1$ up to some cutoff, with critical avalanche-exponent $\delta = 0.35 \pm 0.05$. The parameter-values used are $N_0 = 2$, $g = 1/8$ and $z_c = 6$.

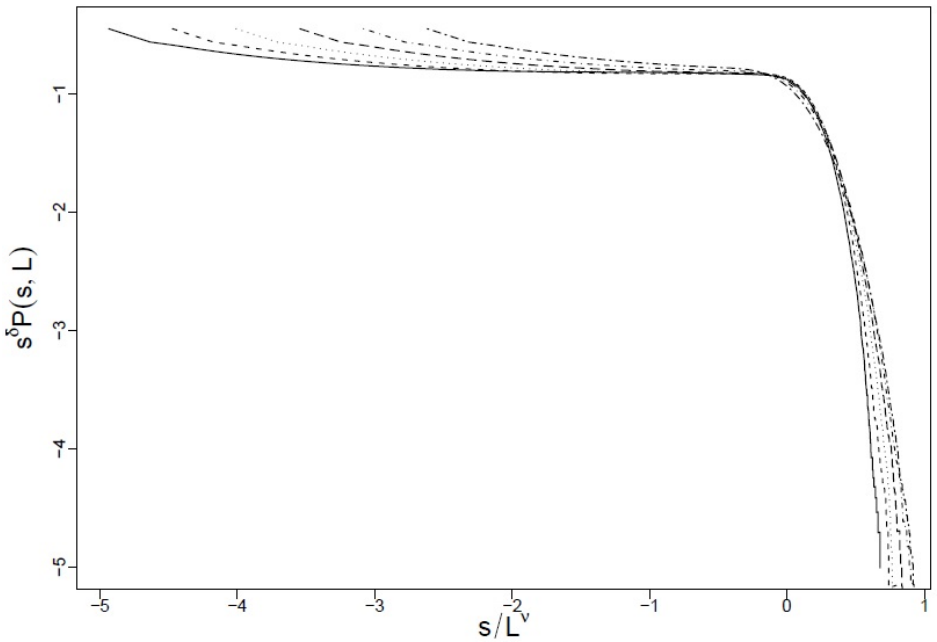


Figure 10: A data collapse of the distributions shown in Fig.9. The data collapse is obtained by plotting the rescaled avalanche-size density $s^{\delta}P(s, L)$ versus the rescaled avalanche size $s/L^{\nu}$, where $\delta = 0.35 \pm 0.05$ and $\nu = 1.54 \pm 0.03$.

Lastly, in Fig. 11, the distributions $P(s, L)$ of avalanches-size $s$ are plotted for the nonlocal-unlimited model. We obtain an avalanche-size exponent $\delta = 0.85 \pm 0.04$ for this model. In Fig. 12, we collapse the data of these distributions by plotting $P(s, L)/s^{-\delta}$ versus $s/L^{\nu}$, where the finite-size scaling exponent $\nu = 2.12 \pm 0.04$ is used.

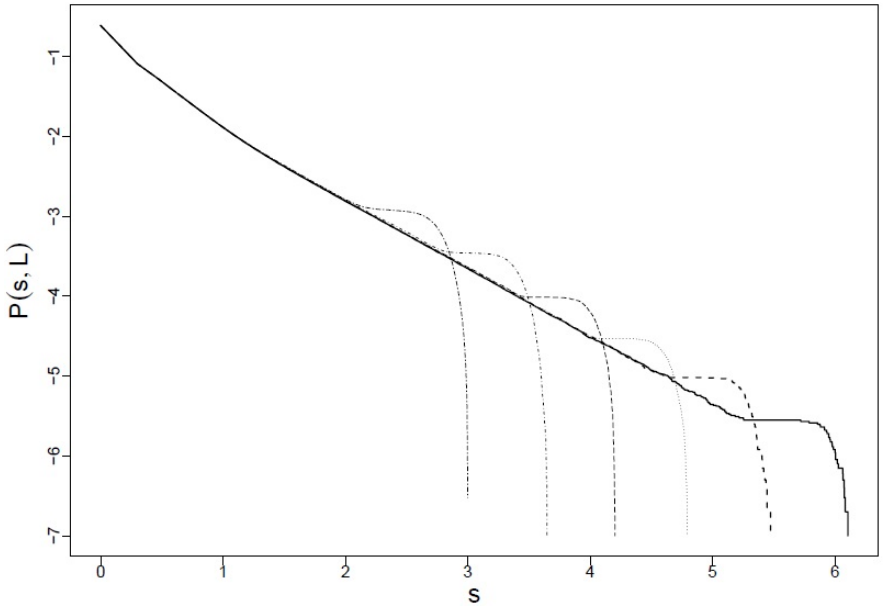


Figure 11: A base 10 log-log plot of the cumulative avalanche-size distributions $P(s, L)$ of the nonlocal-unlimited model for system sizes L = 50,100,200,400,800,1600. The distributions follow a power-law $s^{-\delta}$ for $s >> 1$ up to some cutoff, with critical avalanche-exponent $\delta = 0.85 \pm 0.04$. The parameter-values used are $g = 1/6$ and $z_c = 4$.

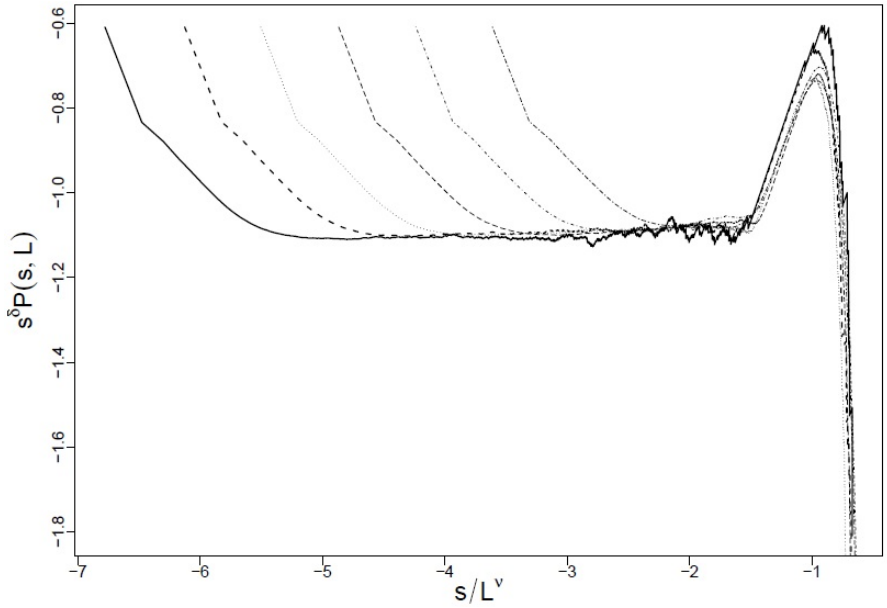


Figure 12: A data collapse of the distributions shown in Fig.11. The data collapse is obtained by plotting the rescaled avalanche-size density $s^{\delta}P(s, L)$ versus the rescaled avalanche size $s/L^{\nu}$, where $\delta = 0.85 \pm 0.04$ and $\nu = 2.12 \pm 0.04$

### 4.2.3 Exponents based on timelife of avalanches

When defining the size of an avalanche according to its timelife $T$, that is, the number of declarations of new active sites during relaxation, we observe significantly different power-law behaviour in both the limited models and the nonlocal-unlimited model. These distributions seem to be well described by the following power-law form

$$P(T, L) = T^{-\rho} g(T/L^{\sigma}), \tag{4.2.4}$$

similar to the ansatz in Eq.(4.1.1). For the same reasons as those stated in section (4.1), we will use the cumulative distribution $P(T, L) = T^{-\gamma} F(T/L^{\sigma})$, where now $\gamma = \rho - 1$. From conservation of probability, we obtain the following relation between critical exponents

$$\int P(s, L)ds = \int P(T, L)dT \;\longrightarrow\; \nu(\tau - 1) = \sigma(\rho - 1) \;\longrightarrow\; \nu\delta = \sigma\gamma, \tag{4.2.5}$$

from which, in addition to $\langle T \rangle$ and $\langle T^2 \rangle$, estimates of the finite-size scaling exponents $\sigma$ can be obtained. Similar data collapses to those shown in section (4.2.2) were observed in all three models. In this section, however, we will only show the observed cumulative distributions $P(T, L)$ and state the values of the critical exponents $\gamma$ and $\sigma$.

In Fig. 13, the cumulative distributions $P(T, L)$ of avalanche lifetime $T$ are plotted for the local-limited model. The finite-size scaling exponents for the local-limited model are $\gamma = 0.85 \pm 0.02$ and $\sigma = 1.43 \pm 0.03$.

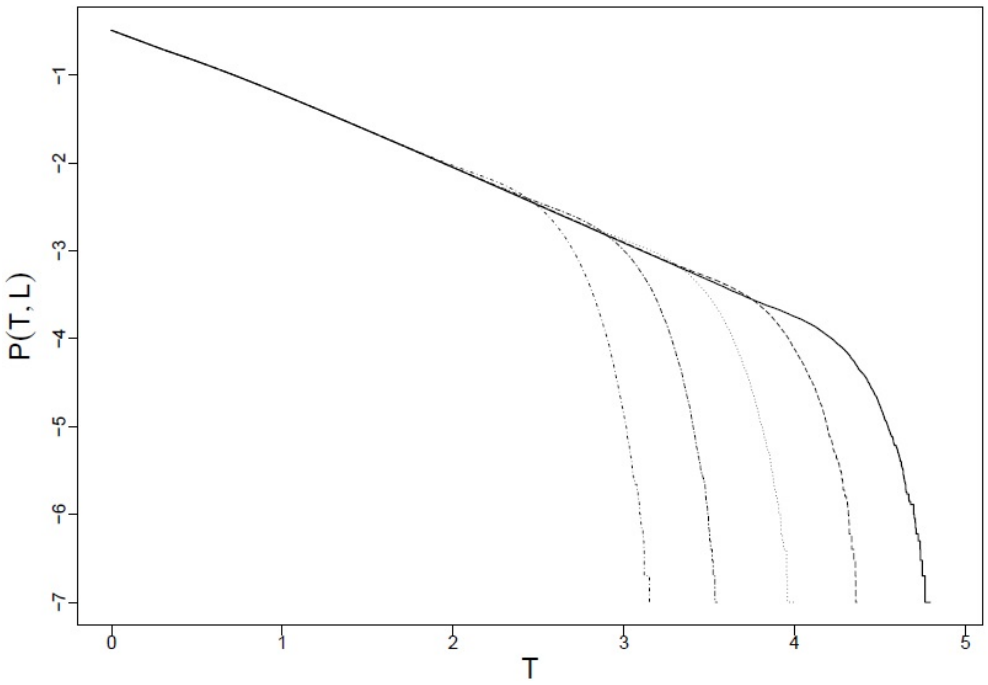


Figure 13: A base 10 log-log plot of the cumulative avalanche-size distributions $P(T, L)$ of the local-limited model for system sizes L = 50,100,200,400,800. The distributions follow a power-law $T^{-\gamma}$ for $T >> 1$ up to some cutoff, where the critical avalanche-exponent is $\gamma = 0.85 \pm 0.02$. The parameter-values used are $N_0 = 2$, $g = 1/8$ and $z_c = 6$.

In Fig. 14, the cumulative distributions $P(T, L)$ of avalanche lifetime $T$ are plotted for the nonlocal-limited model. In this model, the timelife exponent is $\gamma = 0.53 \pm 0.01$, and the finite-size exponent is $\sigma = 1.02 \pm 0.04$.

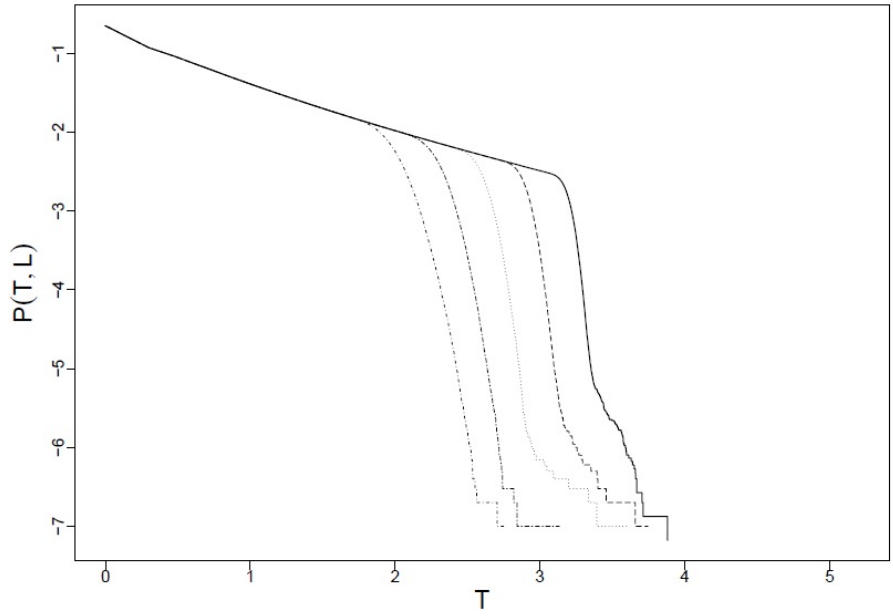


Figure 14: A base 10 log-log plot of the cumulative avalanche-size distributions $P(T, L)$ of the nonlocal-limited model for system sizes L = 100,200,400,800,1600. The distributions follow a power-law $T^{-\gamma}$ for $T >> 1$ up to some cutoff, where the critical avalanche-exponent is $\gamma = 0.53 \pm 0.01$. The parameter-values used are $N_0 = 4$, $g = 1/8$ and $z_c = 6$..

Lastly, in Fig. 15, the cumulative distributions $P(T, L)$ of avalanche lifetime $T$ are plotted for the nonlocal-unlimited model. In this model, the timelife exponent is $\gamma = 1.18 \pm 0.03$, and the finite-size exponent is $\sigma = 1.53 \pm 0.03$.

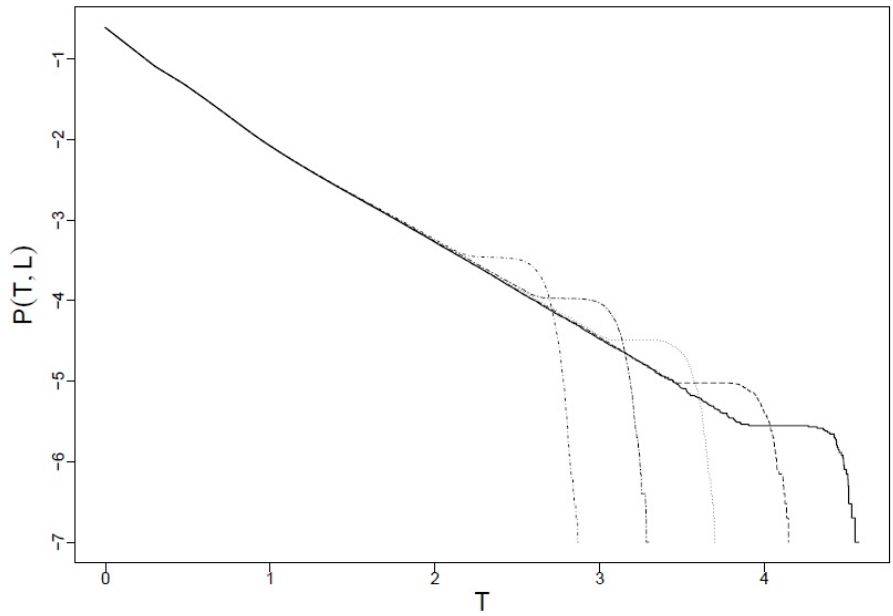


Figure 15: A base 10 log-log plot of the cumulative avalanche-size distributions $P(T, L)$ of the nonlocal-unimited model for system sizes L = 100,200,400,800,1600. The distributions follow a power-law $T^{-\gamma}$ for $T >> 1$ up to some cutoff, where the critical exponent $\gamma = 1.18 \pm 0.03$. The parameter-values used are $g = 1/8$ and $z_c = 6$..

### 4.2.4 Exponents based on number of dropped particles

As mentioned in section (3.3), there arises a difference in the avalanche-size exponent of the nonlocal-unlimited model when we define the avalanche-size as the total number of particles that drop during relaxation versus the total number of topplings during relaxation. The obtained distributions and data-collapse are similar to those shown in Fig. 10 and Fig 11 when considering the total number of particles that drop during relaxation, but the critical exponents now become $\delta = 0.70 \pm 0.03$ and $\nu = 2.54 \pm 0.04$. The exponents of both the limited models of course remain unchanged due to the constant number of particles $N_0$ that fall in a single toppling event.

## 4.3 Differences in avalanche-exponents

All three models thus give rise to different critical exponents, both when using the number of topplings $s$, and the timelife $T$. When looking at the avalanche-exponents of the nonlocal-limited model, we see that these are lower than those seen in the local-limited model. We suspect that this results from the fact that a single toppling event activates more active sites in the nonlocal-limited case as compared to the local-limited case. However, we find that the avalanche-exponents of the nonlocal-unlimited model take on a higher value than those of the local-limited model. This can be explained by looking at the average slope of the steady states, which is approximately equal in the nonlocal, and local-limited model, but differs significantly in the nonlocal-unlimited model. In Fig. 16, the distributions of the occurrence of slopes in the steady states of all three models is shown. As can be seen, the distribution of the nonlocal-unlimited model decays almost exponentially for higher slopes. This implies that the number of particles that fall in a single toppling event will not be very high on average, but also that the probability with which new active sites topple is, on average, significantly lower than that of the other models. Although this model is thus governed by nonlocal rules, the exponents still become higher.

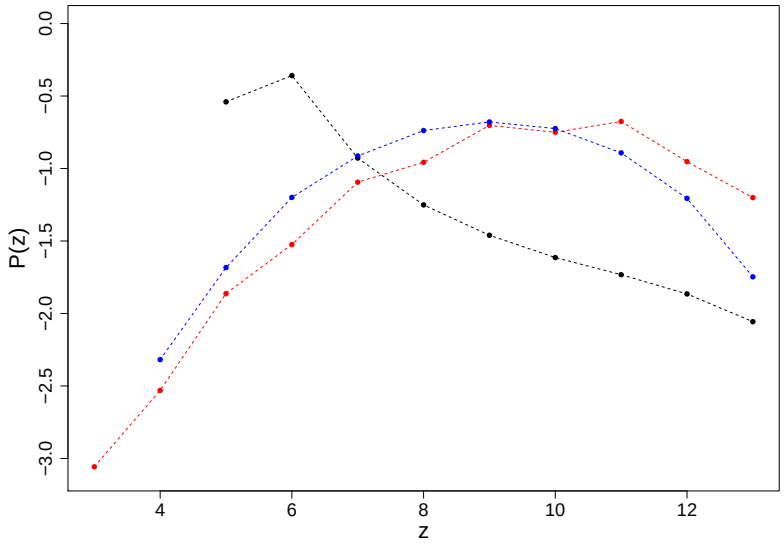


Figure 16: A base 10 semi-log plot of the probability distributions $P(z)$ of observing a slope $z$ in the steady states. The red points represent the local-limited model, the blue points the nonlocal-limited model and the black points the nonlocal-unlimited model. All data is obtained for $L = 200$, $N_0 = 2$, $g = 1/8$ and $z_c = 6$.

# 5 Existence of universality

In this section, we investigate whether the critical behaviour emerging in one or more of our models is universal, that is, can we find a class of different models that exhibit similar critical behaviour, and thus share the same set of critical exponents. The existence of such universality classes requires a certain robustness in the critical behaviour exhibited by the models, which means that the relevant critical exponents, defining the critical behaviour and characterizing the universality class, must not change under variation of certain parameters. Additionally, two models with different parameter-values that exhibit similar critical behaviour must not be trivially the same if one wishes to make conclusions about the critical behaviour being universal. In general, two models can be considered different if their respective raw data is non-identical. Two models exhibiting similar critical behaviour, but non-identical raw data, can thus be regarded as two different models lying within the same universality class. Of course, we already found certain ranges of the parameters $g$, $N_0$ and $z_c$ for which the critical behaviour of our models remains unchanged, and we find that the raw data of these models isn't necessarily identical. However, we could argue that these models are only trivially different, as they are still governed by the same dynamical rules in each case, and differ only in their respective parameter-values. In order to investigate models that are more non-trivially different, we introduce a "flow-parameter", with which we flow from one model to the other. This can be done in a continuous manner when moving from the nonlocal-unlimited model to both the limited models or vice versa. However, this can only be done in a discrete manner when moving between the limited models, in which the number of steps depends on the number of particles $N_0$ that fall in a single toppling event. Introducing such a flow-parameter thus allows us to investigate more non-trivially different models, as all models encountered during a flow are governed by different dynamical rules. The exponents emerging from the dynamics of the models encountered during this evolution are calculated for every step of the flow-parameter, and one can speak of the required robustness in the critical behaviour if this behaviour remains unchanged under a significant range of values of this flow-parameter. If this is the case, we can conclude that we found a class of different models, all exhibiting similar critical behaviour characterized by the relevant critical exponents. In our case, this set of exponents will be formed by the avalanche-exponents $\delta, \gamma$ and finite-size scaling exponent $\nu, \sigma$ defined above, where the avalanche-sizes are thus taken as $\mathrm{s}_{\mathrm{top}}$ and $T$.

## 5.1 Moving in between two models

In order to investigate the existence of universality, we will move from the nonlocal-unlimited model to both the limited models, and from the local-limited model to the non-local limited model. Again, since the critical behaviour emerging from the dynamics of the local-unlimited model is not convincing enough, this model will be left out in the analysis.

### 5.1.1 The flow-parameter

In moving from model $A$ to model $B$, the flow-parameter $p$ is defined as to take on values in the interval $p \in [0, 1]$, where the value $p = 0$ corresponds to model $A$, and $p = 1$ to model $B$. We

will start by letting model $A$ represent the nonlocal-limited model, and model $B$ the nonlocal-unlimited model. In this case, the value of the flow-parameter corresponds to the fraction of the difference between the number of particles that falls according to the nonlocal-unlimited rules, and the number of particles that fall in the nonlocal-limited model. To be more precise, if $N_{NU}$ particles fall in a single toppling event according to the nonlocal-unlimited rules, and $N_0$ particles fall in a single toppling event in the nonlocal-limited case, $N_p = N_0 + p \cdot (N_{NU} - N_0)$ particles will fall in a single toppling event in the model with parameter-value $p$, where $N_p$ is rounded to the nearest integer. Note that all particles still fall according to the nonlocal rules in Eq.(2.1.3). Also note that, in the nonlocal-limited model, $N_0$ particles fall in a single toppling event, whereas in the nonlocal-unlimited model $N_{NU}$ fall. It thus could occur that, according to the nonlocal-unlimited rules, less than $N_0$ particles will fall in a single toppling event. If this is the case, we let $(1 - p)$ be the probability with which $N_0$ particles will fall, and $p$ is thus the probability with which $N_{NU}$ particles fall. In flowing from the nonlocal-unlimited to limited model, we set the other parameter-values to $g = 1/8$, $N_0 = 2$ and $z_c = 6$.

The flow between the nonlocal-limited model and the nonlocal-unlimited model is presented in Fig 17, where the calculated avalanche-size exponents $\delta$ of the models encountered during this evolution are plotted against the corresponding value of the flow-parameter $p$.

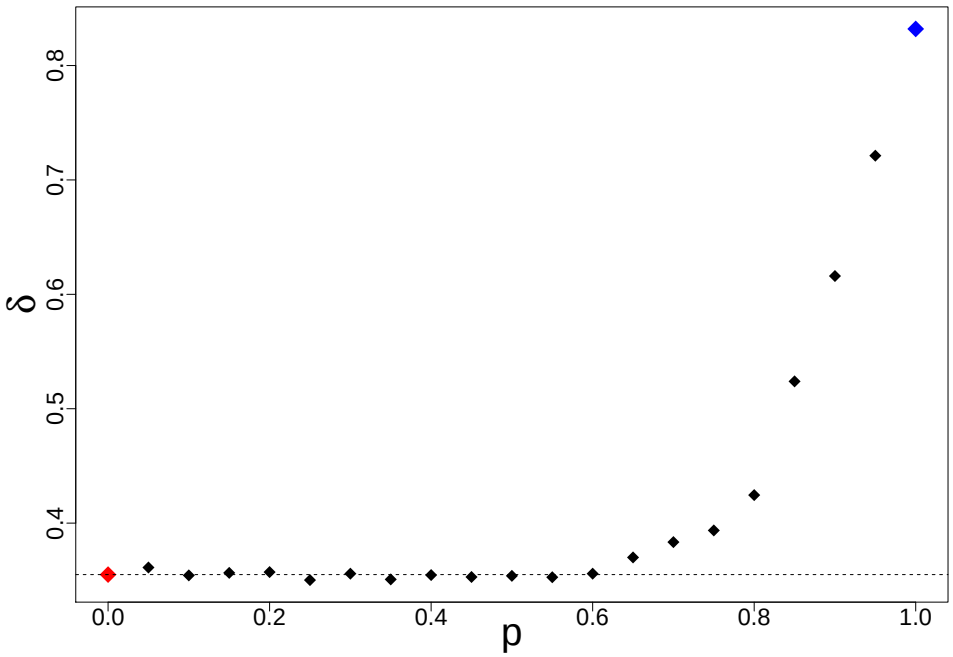


Figure 17: A plot of the avalanche-size exponents $\delta$ of $s^{-\delta}$ of the models that are encountered when flowing between the nonlocal-limited and the nonlocal-unlimited model. The exponents shown are calculated for models that correspond to parameter-values which are seperated by a value of 0.05 in parameter-space. The red data point represents the exponent of the nonlocal-limited model, and the blue data point that of the nonlocal-unlimited model. The constant dashed line drawn through the exponent of the nonlocal-limited model makes it clear that the exponents remain relatively constant in the interval $p \in [0, 0.6]$. The exponents are calculated for system-sizes $L = 1000$, and the parameter-values used are $g = 1/8$, $N_0 = 2$ and $z_c = 6$

As can be seen, the exponents remain relatively constant for a significant range of the flow-parameter, namely $p \in [0, 0.6]$. This shows that the critical behaviour emerging from the dynamics of the nonlocal-limited is robust under variation of the flow-parameter, and that we indeed obtain a class of models which exhibit similar critical behaviour. Furthermore, the raw-data of the models lying within this class is non-identical, at least for flow-parameter values which are seperated by 0.05 in parameter-space. If we thus have some model $C$ with corresponding flow-parameter value $p_c \in [0, 0.6]$, and some model $D$ with corresponding flow-parameter value $p_d \in [0, 0.6]$, then the raw data of these models is non-identical if $|p_c - p_d| \geq 0.05$, implying that the number of particles $N_p$ that fall in a single toppling event, and therewith the dynamical rules, are non-identical when defining these models on finite lattices. Whether models lying closer to each other in parameter-space can be considered as fundamentally different is uncertain. Of course, two models $i$ and $j$, with corresponding parameter-values $p_i$ and $p_j$ that lie very close to each other, are not necessarily different for finite systems. However, since the number of particles that can fall in a single toppling event in the nonlocal-unlimited model scales as $\sim L^{0.354 \pm 0.001}$, as discussed in section (3.2.2), two models $i$ and $j$ with differing parameter-value $p_i$ and $p_j$ are probably different in the limit $L \to \infty$. We can, however, not state this with certainty, but we could argue that, two models $i$ and $j$ which are serepated by a reasonable distance $|p_i - p_j|$ in parameter-space, and that already have non-identical raw data for finite systems, are definitely fundamentally different. In this sense, we thus found a class of different models exhibiting critical behaviour similar to that of the nonlocal-limited model. In addition to the exponents $\delta$ remaining unchanged in the interval $p \in [0, 0.6]$, the finite-size scaling exponents $\nu$ are also similar to that of the nonlocal-limited model $\nu = 1.54 \pm 0.03$ in this interval, emphasizing the similarity in critical behaviour of these models.

Since the critical behaviour arising in the nonlocal-limited model thus seems robust under variation of the flow-parameter $p$, we expect to see a similar robustness in this behaviour when flowing between the nonlocal-limited model and the local-limited model. To test this, we introduce a new flow-parameter $q$, which allows us to flow in between these two limited models. In this case, the value of this flow-parameter $q$ corresponds to the fraction of $N_0 - 1$ particles that will fall nonlocal, where $q = 0$ thus corresponds to the local-limited model, and $q = 1$ to the nonlocal-limited model. Of course, in the case of $N_0 = 2$, the two models are only seperated by one discrete step when using this definition of the flow-parameter. However, since the critical behaviour of both models remains unchanged under variation of the values $N_0 = 2, 3, 4$, we set $N_0 = 4$. This allows us to "flow" between the local-limited and the nonlocal-limited model in three discrete steps. Note that the fraction $q$ is taken over $N_0 - 1$ particles, as one particle always falls local by definition. Also note that the particles that do not fall nonlocal are dropped locally. The number $N_L$ of particles that fall local, and the number $N_{NL}$ of particles that fall nonlocal, thus always satisfy $N_L + N_{NL} = N_0$ in all the models encountered during this flow.

In Fig 18, the avalanche-size exponents $\delta$ of the models corresponding with these three discrete cases are plotted against the flow-parameter $q$. As can be seen, the exponent $\delta$ takes on a similar value in all models, except in the local-limited model $q = 0$. Similarly, the finite-size exponent $\nu$ takes on a similar value in all models for which $q \neq 0$. This again demonstrates the robustness, and therewith the universal nature, of the critical behaviour emerging from the nonlocal-limited dynamics, and confirms the existence of a universality class characterized by these critical exponents. Furthermore, the raw data of all four models is non-identical, and since every model is governed by differing dynamical rules, we can ascertain that these models indeed all are fundamentally different.

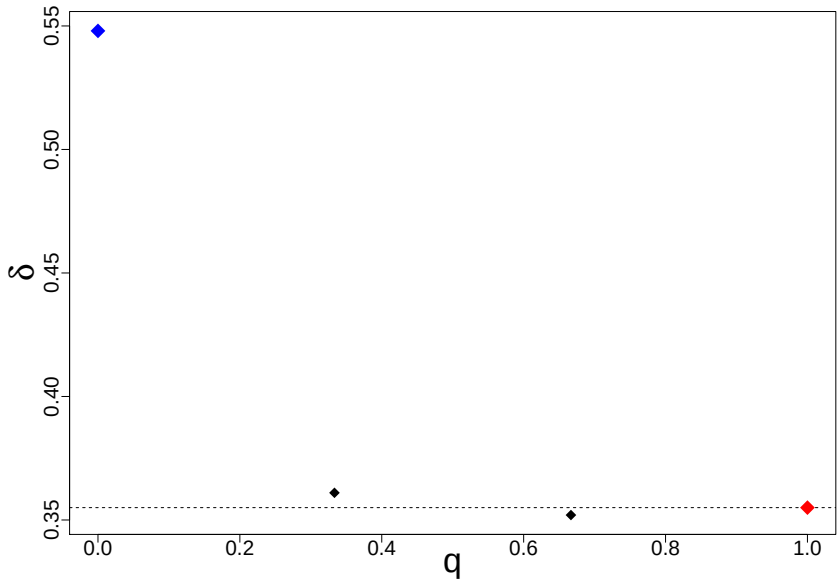


Figure 18: A plot of the avalanche-size exponents $\delta$ of $s^{-\delta}$ of the four models encountered when flowing between the nonlocal-limited and the local-limited model. The exponents shown are calculated for models that correspond to parameter-values $q = 0, 1/3, 2/3, 1$. The red data point represents the exponent of the nonlocal-limited model, and the blue data point that of the local-limited model. The constant dashed line drawn through the nonlocal-limited model illustrates the relatively similar values of the exponents of the models with corresponding parameter-values $q = 1/3, 2/3$. The exponents are calculated for system-sizes $L = 1000$, and the parameter-values used are $g = 1/8$, $N_0 = 4$ and $z_c = 6$

Both the flow with $p$ and $q$ thus suggest that the critical behaviour emerging in the nonlocal-limited model is universal between a class of different models. To even further examine this seemingly universal behaviour, and possibly broaden the set of exponents characterizing this *nonlocal-limited* universality class, we perform the same analysis with the distributions based on lifetime $T$. The flow between the nonlocal-unlimited and nonlocal-limited model is presented in Fig 19, where the calculated avalanche-size exponents $\gamma$ of $T^{-\gamma}$ of the models encountered during the evolution are plotted against the corresponding value of the flow-parameter $p$. As can be seen, the plot almost coincides with the plot in Fig. 17, and the exponents again remain relatively constant in the interval $p \in [0, 0.6]$. Additionally, the finite-size scaling exponents $\sigma$ are also similar to that of the nonlocal-limited model $\sigma = 1.02 \pm 0.04$ in this interval. This assures us that the critical behaviour emerging from the nonlocal-limited model is indeed universal between this class of models, and that these models thus belong to the same universality class.

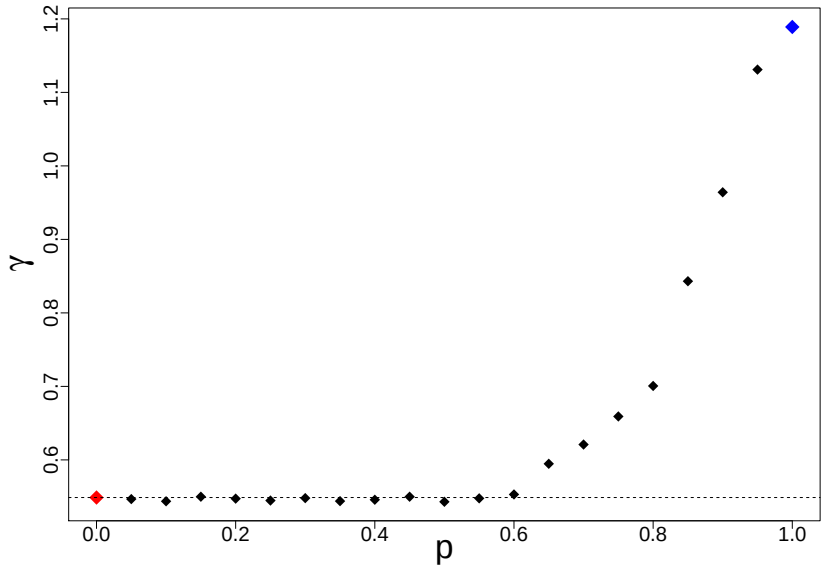


Figure 19: A plot of the avalanche-size exponents $\gamma$ of $T^{-\gamma}$ of the models that are encountered when flowing between the nonlocal-limited and the nonlocal-unlimited model. The exponents shown are calculated for models that correspond to parameter-values which are seperated by a value of 0.05 in parameter-space. The red data point represents the exponent of the nonlocal-limited model, and the blue data point that of the nonlocal-unlimited model. The constant dashed line drawn through the nonlocal-limited model makes it clear that the exponents remain relatively constant in the interval $p \in [0, 0.6]$.

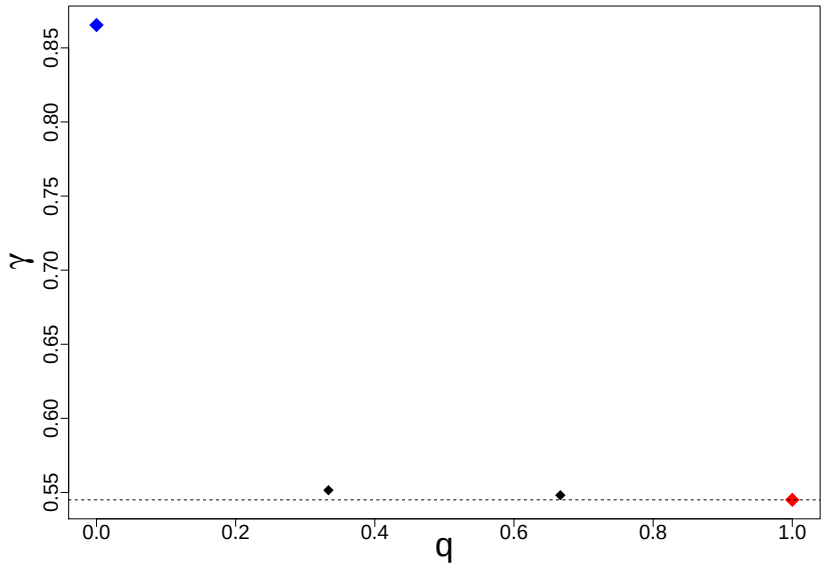


Figure 20: A plot of the avalanche-size exponents $\gamma$ of $T^{-\gamma}$ of the four models encountered when flowing between the nonlocal-limited and the local-imited model. The exponents shown are calculated for models that correspond to parameter-values $q = 0, 1/3, 2/3, 1$. The red data point represents the exponent of the nonlocal-limited model, and the blue data point that of the local-limited model. The constant dashed line drawn through the nonlocal-limited model illustrates the relatively similar values of the exponents of the models with corresponding parameter-values $q = 1/3, 2/3$

In Fig. 20, the flow between the local-limited and nonlocal-limited model is displayed by plotting the timelife-exponents versus the parameter-values $q$ for every distinct model. Again, this plot is very similar to the plot shown in Fig 18, providing convincing evidence that the models with parameter-value $q = 1/3, 2/3$ belong to the same universality class as the nonlocal-limited model. The finite-size exponents $\sigma$ are indeed also similar for these models. Due to this robustness of the critical behaviour arising in the nonlocal-limited model, we expect that the critical exponents of some of the models encountered when flowing between the nonlocal-unlimited and the local-limited model will take on values similar to that of the nonlocal-limited model. We expect this because, when flowing in between these models, some of the models encountered are governed by dynamical rules similar to those of the models with flow-parameter values $q = 1/3, 2/3$. To test this, we flow from the nonlocal-unlimited model to the local-limited model by letting the flow-parameter $h$ simultaneously take on two roles: (i) $h$ acts as the fraction of the unlimited number of particles that will fall nonlocal in a single toppling event, (ii) since only a fraction $h$ of the unlimited particles now falls nonlocal, we simultaneously take a fraction $h$ of the number of particles that *do not* fall nonlocal, and drop these local. In this case, $h = 1$ thus corresponds to the nonlocal-unlimited model, and $h = 0$ to the local-limited model with $N_0 = 1$. Note that there always falls one particle locally by definition, so $h$ is always taken over the $N_{NU} - 1$ particles that would fall nonlocal in the nonlocal-unlimited case. Simulations show, that the models with corresponding flow-parameter values in the interval $h \in [0.2, 0.3]$ indeed take on similar values to that of the nonlocal-limited model for all four exponents $\delta, \nu, \gamma$ and $\sigma$, and thus also seem to lie within the same class. Note that we could also choose to flow by only considering the first role of $h$, but this flow would be very similar to the flow with $p$, and we would therefore probably see something very similar, but now followed by a discrete jump to the local-limited model.

### 5.2 Existence of classes

The results presented above show that the critical behaviour emerging in the nonlocal-limited model remains virtually unchanged over a considerable range of the flow-parameters, and that this behaviour is thus universal between a class of different models. These observations strongly suggest that we have found a new universality class of one-dimensional SOC-models, which is characterized by the set of four critical exponents $\{\delta, \nu, \gamma, \sigma\}$. Furthermore, the invariance of the critical behaviour of the nonlocal-limited model under the variation of the parameters $g$ and $z_c$, over the ranges mentioned in section (2.2), seems to remain for the models lying within the same class, emphasizing the universal nature of this nonlocal-limited behaviour. Because of the dependence of the flow-parameter $p$ on the number of particles $N_0$, we cannot be sure that the range of this parameter under which the critical behaviour remains invariant will be the same when the analysis is performed for other values of $N_0$, at least for finite systems. Of course, the models corresponding to $q = 1/3, 2/3$ only exist for $N_0 = 4$, but one could start with a different value of $N_0$ when flowing with $p$. In doing so, it wouldn't be surprising if one obtains a slightly different range of this flow-parameter $p$ for which the critical behaviour of the models encountered is similar to that of the nonlocal-limited model. This difference, however, will probably vanish in the thermodynamic limit $L \to \infty$. Moreover, the definition of the flow-parameter $h$ is only valid for $N_0 = 1$ in our case. If one thus wishes to use other values of $N_0$ when flowing between the local-limited and nonlocal-unlimited model, this definition has to be adjusted.

# 6 Discussion

## 6.1 Consistency between power-laws and exponential distributions?

As mentioned in section (3.3), there arises a difference in the avalanche-size exponents in the unlimited models when defining the size of an avalanche as the total number of topplings $s_{top}$ occurring during relaxation versus the total number of particles $s_{drop}$ that fall during relaxation. When looking at the distributions of the number of particles that fall in a single toppling event, calculated over all avalanches occurring during a simulation, we observed exponential distributions, as shown in section(3.3.3). Since exponential distributions have a well-defined average, this observation implies that, on average, a fixed amount of particles should fall in a single toppling event. When this is the case, no change in exponents is expected, since, on average, every avalanche with size $s_{drop}$ should be roughly equal to some corresponding avalanche of size $s_{top}$ times this fixed amount of particles. We, however, do see a change in the exponents, which raised the question of whether there possibly exists some inconsistency in the implementations of the unlimited models. Apparently, since the exponent of $s_{drop}$ ($\delta = 0.70 \pm 0.03$) is significantly lower than the exponent of $s_{top}$ ($\delta = 0.85 \pm 0.04$) in the nonlocal-unlimited model, relatively large avalanches occur more often when defining $s$ as $s_{drop}$ compared to $s_{top}$. An intuitive explanation for the coexistence of the exponential distributions and this change in exponents might be the following: in avalanches with a relatively small number $s_{top}$ of topplings, the number of particles that drop in a single toppling event also remains relatively low, whereas in avalanches with a relatively large number $s_{top}$ of topplings, both small and large quantities of particles can fall in a single toppling event. If this is the case, it would imply that the average number of particles $\langle d' \rangle$ that drop in a single toppling event during an avalanche of size $s_{top}$, should grow with $s_{top}$. This is indeed the case in both the unlimited models.

In Fig. 21, this average number of particles $\langle d' \rangle$ that drop in a single toppling event during an avalanche of size $s_{top}$ is plotted on log-log scale against avalanche-size $s_{top}$ for the nonlocal-unlimited model. As can be seen, $\langle d' \rangle$ grows with $s_{top}$, providing a possible explanation for the observed differences in the avalanche-size exponents. Similar behaviour was observed in the local-unlimited model. Although this might serve as an intuitive explanation for the observed differences in the exponents, it is not very rigorous. To really examine whether there exists an inconsistency or not, we will explicitly calculate one distribution from the other in the following section.

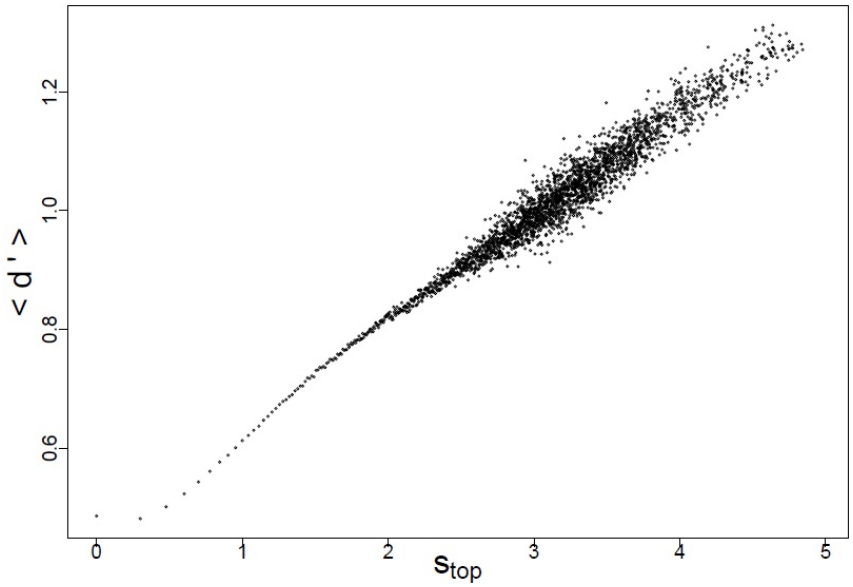


Figure 21: A base 10 log-log plot of the average number of particles $\langle d' \rangle$ that drop in a single toppling event during an avalanche of size $s_{top}$ versus avalanche-size $s_{top}$ for the nonlocal-unlimited model. The data is calculated for $L = 800$, $g = 1/8$ and $z_c = 6$. As can be seen, $\langle d' \rangle$ grows with $s_{top}$. In fact, $\langle d' \rangle$ roughly follows a power-law $\sim s_{top}^{\lambda}$, where $\lambda \approx 0.15$ is approximately equal to the difference of the exponents observed in the distributions of $s_{top}$ and $s_{drop}$.

### 6.1.1 Probability distributions to show consistency

We will investigate the possible inconsistency between the exponential distribution of the number of particles that fall in a single toppling event, and the observed differences in the power-laws for $s_{top}$ and $s_{drop}$, by extracting one distribution from the other with some direct calculations. For simplicity, we let $s_{top} = t$, $s_{drop} = d$, $P_1(t)$ the probability distribution of avalanches in which $t$ topplings occurred, and $P_2(d)$ the probability distribution of avalanches in which $d$ particles fell. Furthermore, we let $P_3(d')$ be the probability of observing $d'$ particles falling in a single toppling event during a simulation, which thus, for the unlimited models, is given by exponential distributions shown on section (3.3.3). To check the consistency between the distributions $P_1(t)$, $P_2(d)$ and $P_3(d')$, we explicitly calculate the distributions $P(x, y)$ and $P(z|w)$, where $x, y, w \in \{t, d\}$, and use the following relations

$$P_1(t) = \int P(t, d)dd, \tag{6.1.1}$$

$$P_2(d) = \int P(t, d)dt, \tag{6.1.2}$$

$$P_3(d') = \int P(d'|w)P_i(w)dw, \tag{6.1.3}$$

where $i$ is thus 1 or 2 depending on $w$, $P(x, y)$ is the joint probability distribution of $x$ and $y$ and $P(z|w)$ is the conditional probability of observing $z$ for given $w$. Indeed, all three equations are satisfied for both the unlimited models, proving that the distributions can coexist and thus no inconsistencies exist between $P_1(t)$, $P_2(d)$ and $P_3(d')$. Apparently, the individual distributions of particle-drops in a single toppling event during an avalanche of size $t, d$, sum to an exponential

distribution when calculated over all occurring avalanches. Note that Eq.6.1.3 only holds for $d' > 0$, as $P_3(0) = 0$, but $\int P(0|w)P_i(w)dw = P_i(0) \neq 0$. The consistency between the distributions shows that the difference in the exponents of the distributions $P_1(t)$ and $P_2(d)$ does not arise from some mistake in the implementations of the model, but really emerges from the dynamics itself. Based on these results, we are tempted to conclude that the intuitive explanation mentioned above is correct, and that the difference in exponents can be explained by the average number $\langle d' \rangle$ of particles dropping in a single toppling event during an avalanche becoming larger with avalanche-size $t, d$.

# 7 Conclusion and outlook

The main objective of this thesis, was to investigate the behaviour emerging through the dynamics of various one-dimensional sandpile models, and to examine whether this behaviour is universal between a class of different models. Furthermore, we addressed the question of whether some critical properties, intrinsic to the steady state itself, could be found, and therewith if the critical behaviour in terms of avalanche-distributions obeying a power-law requires some sort of critical steady state. Firstly, we considered the roughness of the steady states measured in slope-space, and secondly, we studied the possible existence of non-trivial correlations between the slope-variables $z_i$ of these same states. Indeed, we found that the steady state of both the local, and nonlocal-unlimited model exhibits critical behaviour in their roughness as defined in Eq.3.1.2. This criticality manifested itself as a power-law $\sim L^{\alpha}$ of system size $L$ with non-trivial scaling exponents $\alpha$. On the other hand, no non-trivial exponents were found when considering the roughness as defined in Eq.3.1.3, and no non-trivial exponents were found at all in the roughness of the limited models. This observation suggests that the unlimited nature of the dynamics might be one of the main causes for the emergence of non-trivial behaviour in the roughness of a steady state, but further examination is needed to make such statements conclusive. Investigation of the existence of, possibly critical, correlations between the slope-variables $z_i$ was done by means of a slope-slope correlation function as defined in Eq.3.1.4. The resulting data, although not equally convincing in all cases, suggested no correlations existed between the slope-variables. To further test this, we studied various distributions of distances between slope-variables taking on equal, or similar values. These distributions indeed confirmed that no correlations exist in both the limited models, and that the critical avalanche-distributions thus solely emerge through the dynamics in these models. The existence of non-trivial correlations in the unlimited models, however, remains uncertain, as no definite conclusions could be drawn on the resulting data.

In investigating the behaviour emerging from the dynamics of our models, we analysed the distributions of the frequency of occurences of avalanches with avalanche-size $s$. In this analysis, we defined the avalanche-size $s$ in multiple ways: (i) the total number of topplings $\mathrm{s_{top}}$ during relaxation, (ii) the timelife $T$, or number of declarations of new active sites during relaxation, (iii) the total number of particles $\mathrm{s_{drop}}$ that fall during relaxation. In both the limited models and the nonlocal-unlimited model, the analysis led to the identification of critical behaviour in the form of avalanche-distributions following a power-law of avalanche-size $\sim s^{-\delta}$ up to some cutoff. These distributions turned out to be well-described by the finite-size scaling ansatz, allowing for the extraction of two critical exponents per model for a given definition of avalanche-size. The same analysis performed on the local-unlimited model did not lead to the extraction of critical exponents when proposing the finite-size scaling ansatz. This, however, does not necessarily imply that no critical behaviour can be identified with the use of a different analysis, or with different definitions of avalanche-size, but we did not attempt to investigate this further. After establishing critical behaviour based on the extracted critical exponents, we addressed the question of whether this behaviour is universal between a class of different models. This question was addressed by introducing certain flow-parameters, with which we flowed from one model

to the other. Introducing these flow-parameters allowed us to investigate a class of models, all governed by different dynamical rules, for which critical exponents again could be obtained with the use of the finite-size scaling ansatz. Indeed, we found a class of different models exhibiting critical behaviour similar to that of the nonlocal-limited model, and therewith identified a new universality class of one-dimensional models displaying self-organized criticality. Furthermore, investigation showed that the critical behaviour of the models lying within this class also remains invariant under variation of the parameters $g$ and $z_c$, over the ranges mentioned in section 2, emphasizing the universal nature of the nonlocal-limited behaviour. All in all, we thus found critical behaviour in the form of avalanche-distributions obeying a power-law in three of the four models investigated, found critical properties intrinsic to the steady state itself in both the unlimited models, found that the power-law distributions emerge solely through the dynamics in the limited models, and identified a new universality class, characterized by the set of the four critical exponents $\{\delta, \nu, \gamma, \sigma\}$.

## 7.1 Outlook

With regards to future research, several points might come to mind, both concerning the concept of self-organized criticality in general, and the results presented in this thesis. When considering the critical roughness found in the steady states of the unlimited models, one could try to find the cause of this non-trivial behaviour. When observing the steady states, we notice that certain parts often display a relatively large variation in the values of the slope-variables $z_i$, where other parts are formed by a chain of consecutive slope-variables $z_i = z_c$. These non-rough patches thus might, on average, grow with some non-trivial growth-factor, causing a non-trivial growth of the roughness in the unlimited models. Also, no clear conclusions could be drawn on the existence of non-trivial correlations in the steady states of the unlimited models, thus requiring further research. If, however, such non-trivial correlations exist, one could investigate if, and how, these correlations play a role in the emergence of critical avalanche-distributions in the unlimited cases. Furthermore, in equilibrium physics the distribution of the states is given by the well-known Boltzmann distribution. On the other hand, such distributions are generally not known in models displaying self-organized criticality, as these models are often non-equilibrium by definition. Although probably somewhat ambitious, finding such a distribution for the recurrent states of our models according to some scalar quantity arising from a sum over the slope-variables $z_i$ for example, might lead to a better understanding of SOC-models governed by dynamical rules based on height differences in general.

In addition to the suggestions concerning the results of this thesis made above, some suggestions can also be made regarding self-organized criticality in general. For example, to date, there does not exist a set of rules by which one can determine a priori if a system will display SOC or not. Being able to determine beforehand whether an algorithm displays SOC would greatly reduce the time and effort needed for research in this area, and finding such a set of rules would probably lead to a better understanding of the emergence of complexity in certain systems. Furthermore, the calculation of possible universality classes of models displaying SOC is still missing. Although considering these issues is beyond the scope of this thesis, they leave plenty of room for further research into the remarkable world of self-organized criticality.

# 8 Acknowledgements

First and foremost, I would like to thank Bernard Nienhuis for the inspiring weekly discussions and his guidance throughout this project. Holding an A4-paper against my laptop screen, or looking along my laptop screen from the side to check whether a line on the log-log scale really is straight, is something I will remember with pleasure from our meetings. I would also like to thank Jasper van Wezel for his immediate and enthusiastic response when I asked him to be my second assessor, and for his interesting questions during the presentation of my thesis. Lastly, I would like to thank my parents and my cat Jip for their support throughout this final year of my master's degree.

# 9 References

[1] P. Bak, C. Tang, and K. Wiesenfeld, Self-organized criticality: an explanation of 1/f noise. Phys. Rev. Lett.59, 381 (1987); Self-Organized Criticality, Phys. Rev. A, Vol 38 , 364 (1988).

[2] Kadanoff, L.P., Nagel, S.R. Wu, L. & Zhou, S. 1989. Scaling and universality in avalanches. Physical review A, 39.

[3] S. S. Manna, Two-state model of self-organized criticality. J. Phys. A 24, L363 (1991).

[4] Hoai Nguyen Huynh et al.The Abelian Manna model on various lattices in one and two dimensions. J. Stat. Mech. (2011) P09024.

[5] S. B. Lee, Universality class of the conserved Manna model in one dimension. Phys. Rev. E 89, 060101(R) (2014).

[6] S. Kwon, J. M. Kim, Critical behavior of a fixed-energy Manna sandpile model for regular initial conditions in one dimension. Phys. Rev. E 92, 062149 (2015).

[7] T. Becker, H. de Vries, and B. Eckhardt, Dynamics of a Stochastically Driven Running Sandpile. J. Nonlinear Sci. Vol. 5: pp. 167-188 (1995).

[8] K. Christensen, A. Corral, V. Frette, J. Feder, and T. Jossang, Tracer Dispersion in a Self-Organized Critical System. Phys. Rev. Lett. 77, 107 (1996).

[9] A. Malthe-sorenssen, P. Meakin, K. Christensen, V. Frette, J. Feder, and T. Jossang. Avalanche dynamics in a pile of rice. Nature. Vol 379, 49 (1996).

[10] L. A. Nunes Amaral, K. B. Lauritsen, Self-organized criticality in a rice-pile model, Phys. Rev. E 54 (1996).

[11] F. Slanina, Self-organized branching process for a one-dimensional rice-pile mode, lEur. Phys. J. B25, 209216 (2002)

[12] S. Hong-Zhang, T. Zheng-Xin, Critical Behaviors in a Stochastic Local Limited One-Dimensional Rice-Pile Model, Vol. 50, No. 2, August 15, 2008

[13] V. de Carvalho, A. Caparica, R. Dickman. Conserved Sandpile with A Variable Height Restriction. Braz J Phys (2013) 43:254259

[14] R. Dickman, M. Alava, M.A. Munoz, J. Peltola, A. Vespignani, S. Zapperi. Critical behavior of a one-dimensional fixed-energy stochastic sandpile. Phys. Rev. E64, 056104 (2001).

[15] R. Dickman, Critical exponents for the restricted sandpile. Phys. Rev. E73, 036131 (2006).

[16] R. Dickman, J. M. M. Campelo, Avalanche exponents and corrections to scaling for a stochastic sandpile. 2003 Phys. Rev. E67 066111

[17] P. Bak, K. Chen, C. Tang, A forest-fire model and some thoughts on turbulence. Physics Letters A, 1990, Vol.147(5)

[18] M. paczusk, P. Bak, Theory of the one-dimensional forest-fire model. Physcal review E, 1993, Vol 48(5)

[19] B. Drossel, S. Clar, F. Schwabl, Exact results for the one-dimensional self-organized critical forest-fire model. Physical review letters, 1993, Vol 71

[20] B. Drossel, Self-organized criticallity and synchronization in a Forest-fire model, Physical review letters, 1996, Vol 76

[21] V. B. Priezzhev, D. V. Ktitarev, and E. V. Ivashkevich. Formation of Avalanches and Critical Exponents in an Abelian Sandpile Model. Physical review letters, 1996 Vol 76

[22] L.A.N. Amaral, K. B. Lauritsen. Universality classes for rice-pile models. Physical review E, 1997 Vol 76

[23] S N Majumdar, Deepak Dhar. Height correlations in the Abelian sandpile model. J. Phys. A Math. Gen. 24 (1991) L357-L362

[24] M. Kardar, G. Parisi, Y.C. Zhang. Dynamic Scaling of Growing Interfaces. Phys. Rev. Lett. 56, 889

[25] J. Krug, J. E. S. Socolar, and G. Grinstein. Surface fluctuations and criticality in a class of one-dimensional sandpile models. Phys. Rev. A 46, R4479(R)